

NACA RM E51L14

FOR REFERENCE **NACA**

NOT TO BE TAKEN FROM THIS ROOM

RESEARCH MEMORANDUM

ALTITUDE PERFORMANCE INVESTIGATION OF SINGLE- AND
DOUBLE-ANNULAR TURBOJET-ENGINE COMBUSTORS
WITH VARIOUS SIZE FUEL NOZZLES

By James L. Harp, Jr., and Kenneth R. Vincent

Lewis Flight Propulsion Laboratory
Cleveland, Ohio

CLASSIFICATION CHANGED
UNCLASSIFIED

To _____

T. A. C. Res. also

By authority of ** R. N. - 123* Date *effective Dec. 13, 1958*

AMT 1-20-58 CLASSIFIED DOCUMENT

This material contains information affecting the National Defense of the United States within the meaning of the espionage laws, Title 18, U.S.C., Secs. 793 and 794, the transmission or revelation of which in any manner to an unauthorized person is prohibited by law.

NATIONAL ADVISORY COMMITTEE FOR AERONAUTICS

WASHINGTON
June 9, 1952



NATIONAL ADVISORY COMMITTEE FOR AERONAUTICS

RESEARCH MEMORANDUMALTITUDE PERFORMANCE INVESTIGATION OF SINGLE- AND
DOUBLE-ANNULAR TURBOJET-ENGINE COMBUSTORS
WITH VARIOUS SIZE FUEL NOZZLES

By James L. Harp, Jr., and Kenneth R. Vincent

SUMMARY

An investigation of the performance of an annular-combustor-type turbojet engine was conducted, and the performance of a NACA single-annular combustor having controlled air distribution was compared with that of the standard double-annular combustor. The turbine-discharge temperature profiles, combustion efficiency, altitude limits, and engine performance using both combustors were investigated and compared over a range of altitudes and engine speeds at two flight Mach numbers with four sets of fuel nozzles having different flow rates. Duct tests of a one-fourth sector combustor of the single-annular design were used to predict any necessary changes that were made to the full-scale combustor.

The most significant advantage of the single-annular combustor over the double-annular combustor was improved combustion efficiency. However, this gain was not fully realized in engine specific fuel consumption because of the larger pressure loss through the single-annular combustor. The effect of fuel nozzle size on the single-annular combustor using JP-3 was negligible, but the use of small fuel nozzle sizes at high altitudes with the double-annular combustor using gasoline not only prevented temperature inversion, but also provided specific fuel consumptions as low as values obtained with the single-annular combustor. The altitude limits of the single- and double-annular combustors were essentially the same. Combustion efficiency and altitude operational limits with the single-annular combustor were not appreciably affected by changes in fuel volatility. In general, a good agreement existed between the full-scale combustor and the one-fourth sector investigations.

INTRODUCTION

Increased operational altitudes of current aircraft emphasize the need for continued improvements in the altitude limits and altitude performance of current turbojet engines. One disadvantage of turbojet engines is poor fuel economy, which is aggravated by decreasing combustion



efficiency with increasing altitude. Any improvement that can be obtained in combustion efficiency at high altitudes will generally result in improved range or pay load. Combustion blow-out at low engine speeds and limitation of the maximum engine speed due to excessive turbine-gas temperatures for engines equipped with fixed-area exhaust nozzles generally establish the altitude limits of turbojet engines.

The purpose of the investigation conducted at the NACA Lewis laboratory and reported herein was to determine the improvements possible in full-scale turbojet-engine performance when a single-annular combustor with slotted air-inlet orifices was used. The combustors investigated were developed using as a guide the information obtained from a one-fourth sector investigation. Five modifications were made to the original single-annular combustor design, and the modification giving the best performance with regard to outlet radial temperature distribution was compared with the standard engine combustor for the engine investigated. The investigation covered a range of altitudes from 10,000 to 50,000 feet at flight Mach numbers of 0.30 and 0.60. The effect of fuel atomization on combustor performance was investigated by using four sets of fuel nozzles having different flow rates; the effect of the Reid vapor pressure of the fuel was also investigated. Performance comparisons include combustion efficiency, combustor pressure loss, turbine-discharge temperature profiles, turbine-discharge total temperatures, net thrust, and net-thrust specific fuel consumption.

APPARATUS AND PROCEDURE

Altitude Chamber

The altitude-test chamber in which the engine was installed is 10 feet in diameter and 60 feet in length, and is illustrated in figures 1 and 2. The test chamber is divided into three sections separated by steel bulkheads - the air inlet section, the engine compartment, and the exhaust section. The engine was mounted on a thrust measuring bed with the tail-pipe extending through a bulkhead into the exhaust section. Freedom of movement of the inlet duct was provided in an axial direction by means of a labyrinth seal. A rear bulkhead was installed around the engine tail pipe to prevent recirculation of the hot exhaust gases around the engine.

Instrumentation

The locations of the instrumentation stations for the engine are shown in figure 3. The detailed location of the separate temperature and pressure probes at each station is shown in figure 4. The instrumentation at the engine inlet, station 1, was used in calculating the

altitude correction factors θ and δ and the engine air flow. The jet thrust was computed using the pressures and temperatures at stations 6 and 7 (see appendix). The atmospheric pressure surrounding the jet nozzle was sensed by four lip static tubes (fig. 4(f)). The turbine-discharge temperature profiles were determined from the six rakes having eight thermocouples each which are shown in figure 4(d). The turbine-discharge temperature at any given radial immersion is the average of the six thermocouples at that immersion. Fuel flow was measured by rotameters calibrated for the three types of fuels used in this investigation (MIL-F-5572, MIL-F-5624A (JP-3), and a low volatility fuel having a Reid vapor pressure of 1 lb/sq in.). Analysis of fuels used is presented in table I.

Engine

The engine used was a J34-WE-18 axial-flow turbojet engine having an 11-stage compressor giving a pressure ratio of approximately 4 to 1 at the rated engine speed of 12,500 rpm, a double-annular combustor of the through-flow type, and a two-stage axial-flow turbine. For this investigation, the standard engine fuel-control system was removed and an external fuel pump, a pressure regulator, and a fuel throttle were installed. These alterations were made in order that the performance of the engine could be obtained outside the limits imposed by the fuel-control system. These components of the fuel system were retained throughout the investigation.

The standard engine flow divider and the two concentric fuel manifolds are shown schematically in figure 5(a). There are 36 nozzles in the outer manifold and 24 in the inner manifold that supply fuel to the outer and inner annuli, respectively. For the investigation of the standard double-annular combustor, two matched sets of fuel nozzles with 80° cone angles were used, one with a flow rate of 7.0 gallons per hour and the other with a flow rate of 3.0 gallons per hour at a pressure drop of 100 pounds per square inch.

The flow divider and fuel manifold used with the single-annular combustor are shown schematically in figure 5(b). This manifold has eight separate segments with five fuel nozzles mounted in each segment, giving a total of 40 fuel nozzles. The flow divider is a NACA design (reference 1). For the investigation of the single-annular combustor, three matched sets of fuel nozzles with a cone angle of 80° were used with flow rates of 10.5 gallons per hour, 6.0 gallons per hour, and 3.0 gallons per hour at a pressure drop of 100 pounds per square inch. Because the single-annular combustor had only 40 nozzles whereas the double-annular combustor had 60 nozzles, the fuel pressure and atomization of the 7.0- and 3.0-gallon-per-hour nozzles used in the double-annular combustor are approximately equal to the 10.5- and 6.0-gallon-per-hour nozzles used in the single-annular combustors, respectively.

The double-annular combustor used in this investigation is pictured in figure 6 and the single annular combustor model 1, in figure 7. The cross sections of the two combustors are compared in figure 8. It can be seen that the major differences between the two combustors is that one has a single annulus and slotted air admission ports, whereas the other has a double annulus with round and oblong air admission ports.

Several modifications of the single-annular combustor were investigated to obtain a satisfactory turbine-discharge temperature profile. These modifications are shown in figure 9. The basic principle in this combustor design, based on the results of the investigation reported in reference 2, led to admitting air through slotted axial air openings. The air as it flows into the combustor creates alternate air-rich and fuel-rich zones with a zone of combustible mixture between them extending axially throughout the length of the combustor. This method permanently seats the flame at the front of the combustor because any tendency of the flame to move downstream is counteracted by its tendency to spread back upstream through these zones of combustible mixture. The admission of air to the combustor can be controlled by opening or closing slots and thus almost any desired temperature profile can be obtained. In general, opening slots in the inner wall will lower the blade root temperature and closing them will raise the root temperature. The same process holds for the outer wall. Opposing this process, however, is the tendency of the air to penetrate to the opposite wall. Consequently, 13 air baffles or fingers (fig. 9(f)) were installed on the inner wall of model 6 to raise the tip temperature without appreciably affecting the root temperature. Photographs of model 6 are presented in figure 10.

Procedure

The general method followed in this investigation was to determine the performance of the J34-WE-18 engine with its standard double-annular combustor and to compare the results with those of the best of the single-annular configurations, model 6. In order to determine the effects of fuel atomization and spray pattern on engine and combustor performance and thereby simulate duplex or variable-area nozzle operation, data were obtained using 7.0- and 3.0-gallon-per-hour fuel nozzles in the double-annular combustor and 10.5-, 6.0-, and 3.0-gallon-per-hour fuel nozzles in the single-annular combustor.

Inlet and exhaust pressures were set to correspond to the desired flight conditions in the NACA standard atmosphere assuming 100-percent ram pressure recovery. The pressures were set to within ± 1.5 pounds per square foot and, in general, the inlet temperature, to within $\pm 5^\circ$ F. The range of altitudes covered was from 10,000 to 50,000 feet at flight Mach numbers of 0.30 and 0.60. At each flight condition, the engine speed was varied over a range from approximately 4000 to 12,500 rpm.

The altitude operating limits are defined by either combustor blow-out or the specified idling speed limitation at the low speed limit, and by either limiting turbine temperature or rated speed at the high speed limit. The high speed limit is imposed on the engine by turbine-blade stress considerations. This limit is composed of two factors - the physical stress induced by rotation of the turbine wheel and the gas forces, and the lowering of allowable stress limits by high gas temperatures. The dotted curve shown in figure 11 is the temperature limit curve for this engine at maximum rated engine speed. The maximum temperature-limited engine speed was considered reached when the turbine-discharge gas temperature profile became tangent to this design curve at any point, or when an engine speed of 12,500 rpm was obtained.

The performance of the double-annular combustor was obtained with the engine exhaust nozzle sized such that the turbine-discharge temperature profile was tangent to the manufacturer's limiting profile at an engine speed of 12,500 rpm at an altitude of 5000 feet and a flight Mach number of 0. This matching was accomplished with the 7.0-gallon-per-hour fuel nozzles installed, and the resultant exhaust-nozzle area was 181.0 square inches.

With the installation of the single-annular combustor, the higher pressure drop of this combustor required a rematching of the exhaust nozzle to the engine. In order that the engine performance data with the two combustors be directly comparable, it was desirable that the engine exhaust-nozzle area with the single-annular combustor be sized to produce limiting temperature at rated engine speed at an altitude of 5000 feet and a Mach number of 0, as was done with the double-annular combustor. However, the single-annular combustor had not been developed sufficiently to assure adequate life and was therefore run only at the higher altitudes where the least stress would be imposed on the basket. The exhaust-nozzle area had therefore to be estimated instead of sized experimentally. The area used was 194.1 square inches. Upon completion of the single-annular combustor investigation, it was found that limiting temperature did not occur at rated speed for the lowest altitude (20,000 feet) investigated. Consequently, the engine performance data with the single-annular combustor had to be adjusted to values that would have been obtained had the nozzle area been such that, at an altitude of 20,000 feet and a Mach number of 0.60, limiting temperature would have occurred at the same engine speed at which limiting temperature occurred with the double-annular combustor. This speed was 12,615 rpm, which is slightly over rated speed for the engine. The exhaust-nozzle area should have been 196.0 square inches instead of 194.1 square inches. The method used to adjust the data in this manner is explained in detail in the appendix.

Performance with the double-annular combustor was determined with MIL-F-5572 (clear gasoline) as the fuel; performance with the single-annular combustor was determined with MIL-F-5624A, grade JP-3. A short investigation was also made with the single-annular combustor using a special fuel with a Reid vapor pressure of 1 pound per square inch for comparative purposes.

A one-fourth sector combustor of the single-annular design placed in a duct was used to predict any necessary changes that were to be made to the full-scale combustor. Agreement between the sector and full-scale combustors was generally good.

RESULTS AND DISCUSSION

Design Considerations

In selecting the best NACA single-annular combustor configuration for comparison with the standard double-annular combustor, the turbine-discharge temperature profile as well as combustion efficiency, combustor pressure loss, and altitude limits was considered. Turbine-discharge temperature profiles are shown for representative single-annular combustor configurations in figure 11. The manufacturer's temperature limit is shown in this figure as the dashed curve. Of the six configurations investigated, model 6 (containing the 13 fingers) provided a temperature profile nearest that of the manufacturer's limiting profile.

Combustion efficiency and pressure loss for the NACA configurations are compared in figures 12(a) and 12(b). Model 6 had the highest combustion efficiency, but it also had the highest pressure loss. Nevertheless, considerations of all three of these parameters indicated that because of the better temperature profile and hence higher average tail-pipe temperature, and because of the higher combustion efficiency, configuration 6 would provide the best over-all performance. All subsequent single-annular combustor performance data are for configuration 6.

Turbine-Discharge Temperature Profiles

Temperature profiles with the standard double-annular combustor are shown in figure 13 for a range of altitudes at the temperature-limited engine speed. These data were obtained with both 7.0-gallon-per-hour and 3.0-gallon-per-hour fuel nozzles in order to determine the effects of fuel spray characteristics on performance. In most cases, the points shown in this figure have been interpolated from data obtained over a range of engine speeds because of the difficulty in setting engine conditions such that the observed profile would coincide with the limiting profile at least at one point. As can be noted in figure 13(a), a

temperature inversion occurred which shifted the peak temperatures toward the turbine blade root with increased altitudes for the standard fuel nozzles. This inversion required a decrease in temperature-limited speed and average tail-pipe temperature with increasing altitude to avoid exceeding turbine temperature limits. The inversion is attributed in part to the effect of the compressor-discharge velocity profile on the combustor. As altitude and consequently corrected engine speed were increased, the velocity gradient became severe with high velocity at the tip and low velocity at the root.

Installing the 3.0-gallon-per-hour fuel nozzles in the double-annular combustor for high altitude operation to simulate duplex or variable-area-type fuel nozzles essentially eliminated this inversion. The profile at 45,000 feet was very similar to the profile at 10,000 feet with the 7.0-gallon-per-hour nozzles. This result apparently is due to better fuel penetration into the incoming air.

Data for a later model of this engine indicate that a flow mixer installed at the compressor outlet eliminates the temperature inversion using the 7.0-gallon-per-hour fuel nozzles. The flow mixer did not improve the basic low altitude temperature profile, but did maintain the basic low altitude temperature profile as altitude and corrected engine speed were increased. An example of the effectiveness of such a device is shown by the data in figure 14. The serious inversion encountered at high corrected engine speeds was essentially eliminated with the mixer installed.

Profiles of the single-annular combustor model 6 with 10.5-, 6.0-, and 3.0-gallon-per-hour fuel nozzles are shown in figure 15 over a range of altitudes at the temperature-limited engine speed. The 10.5-gallon-per-hour nozzles gave approximately the same engine fuel flows as the 7.0-gallon-per-hour nozzles in the double-annular combustor for a given fuel pressure. The combustor was considerably less sensitive to compressor-discharge velocity profile than the double-annular combustor. With the 10.5-gallon-per-hour nozzles there was no inversion up to 40,000 feet, but a moderate change was apparent at 50,000 feet.

Combustion Efficiency

The combustion efficiency of the double-annular combustor is shown in figure 16 for three altitudes with the standard 7.0-gallon-per-hour fuel nozzles and the 3.0-gallon-per-hour nozzles. There was considerable reduction in efficiency with the standard nozzles as the altitude was

increased, particularly at reduced engine speed. Using the smaller nozzles to simulate variable-area type nozzle operation at altitude resulted in an increase in combustion efficiency of more than 20 percent at altitude cruising conditions, indicating the desirability of using variable-area or duplex-type nozzles in the standard combustor. On the other hand, the single-annular combustor was relatively insensitive to changes in fuel nozzle size, as shown in figure 17.

As illustrated by the comparison in figure 18, the combustion efficiency of the single-annular combustor was higher than that of the double-annular combustor at all conditions, except for high engine speed at an altitude of 20,000 feet where the efficiencies were approximately equal. With the standard 7.0-gallon-per-hour fuel nozzles in the double-annular combustor using gasoline as fuel, combustion efficiency at cruising engine speed at an altitude of 50,000 feet was as much as 30 percent lower than that of the single annular combustor operating on JP-3 fuel. Although data for a direct comparison are not available, the data presented in figure 16 indicate that use of the 3.0-gallon-per-hour nozzles in the standard combustor would reduce the differences in efficiency to less than half those shown in figure 18 with the large fuel nozzles.

The performance of the single-annular combustor, which was designed for grade JP-3 fuel, was also evaluated using a modified JP-3 fuel having the light ends removed so as to reduce the Reid vapor pressure from 7 to 1 pound per square inch. Comparison of the combustion efficiencies in figure 19 shows essentially no effect for this change in fuel.

A previous investigation (reference 3) during which both gasoline and JP-3 fuel were used in the double-annular combustor showed that combustion efficiency with JP-3 fuel was from 5 to 20 percent lower than with gasoline.

Combustor Pressure Loss

Combustor pressure loss was generalized by the method of reference 4 and is shown in figure 20. Data obtained with all fuel nozzles are presented for both combustors over a range of altitudes. The single-annular combustor had more than twice the pressure loss of the standard double-annular combustor. Effect of this pressure loss on performance will be discussed in a later section.

Altitude Operating Limits

The altitude operating limits are defined by either combustor blow-out or idling limitation at the low speed limit, and by either limiting turbine temperature or rated speed at the high speed limit. Altitude

limits of the double-annular combustor at a Mach number of 0.30 with the 3.0- and 7.0-gallon-per-hour fuel nozzles are shown in figure 21. With the standard nozzles, the maximum altitude was 50,000 feet; the limit for the small nozzles was generally slightly higher. At a Mach number of 0.30 while using the 7.0-gallon-per-hour fuel nozzles, a region of unstable and rumbling combustion was encountered. It is believed that this rumbling was possibly due to an intermittent lighting and extinguishing of the inner annulus or an instability in the combustor which was aggravated by resonant characteristics of the altitude chamber. This belief appears logical because unstable combustion was not encountered at any altitude or Mach number with the 3.0-gallon-per-hour fuel nozzles nor at a flight Mach number of 0.60 with the standard fuel nozzles, and no such phenomenon has been reported elsewhere from flight tests.

The altitude limits for the single-annular combustor at a flight Mach number of 0.60, shown in figure 22, were essentially unaffected by fuel nozzle size. The maximum altitude obtainable with this combustor was approximately 55,000 feet. No unstable operation was encountered with the single-annular combustor.

Comparing the double- and single-annular combustors at a Mach number of 0.60 with 7.0- and 10.5-gallon-per-hour fuel nozzles, respectively (fig. 23), indicates that the altitude limits were about the same at cruising and high speed operating conditions. Below an altitude of 50,000 feet it was sometimes possible to reduce the speed with the double-annular combustor by as much as 2200 rpm below the blow-out speed for the single-annular combustor. This region of operation is unimportant, however, except possibly for aircraft let-down operation.

The altitude limits of the single-annular combustor using high and low volatility fuels were essentially unaffected, as shown in figure 24. Using gasoline and JP-3 fuel in the double-annular combustor (reference 3) indicated that the altitude limits of the double-annular combustor similarly were not appreciably affected by a change in fuel volatility.

ENGINE PERFORMANCE

Variation of corrected net thrust with corrected engine speed is presented in figure 25 for the single- and double-annular combustors. Ticks on the curves indicate the temperature-limited engine speeds and thrusts for both combustors. At a given engine speed, the thrust with the two combustors was essentially the same except at an altitude of 50,000 feet. At a given engine speed (fig. 26) the tail-pipe temperature with the single-annular combustor was higher than that of the standard double-annular combustor because of an improved turbine temperature profile, but no gains in thrust were realized (fig. 25) with the

single-annular combustor because of the high pressure drop through that combustor. At an altitude of 20,000 feet and a Mach number of 0.6, the limiting temperature for both combustors occurred at approximately rated engine speed. At an altitude of 40,000 feet and Mach numbers of 0.30 and 0.60, the temperature-limited engine speeds and hence maximum net thrusts were slightly higher for the single-annular combustor because of an improved turbine temperature profile. However, at an altitude of 50,000 feet, the single-annular combustor began to suffer the effects of temperature inversion (fig. 15), that is, a reduction in temperature-limited engine speed and average tail-pipe temperature. These effects, combined with the higher pressure loss, caused both the maximum thrust obtainable and thrust at a given engine speed to be lower than that obtained with the double-annular combustor.

Installation of a flow mixer at the compressor outlet to eliminate temperature inversion in the double-annular combustor would probably eliminate any margin in maximum thrust of the single-annular combustor over the double-annular combustor.

Variation of net-thrust specific fuel consumption with corrected engine speed, presented in figure 27, indicates that the specific fuel consumption of the single-annular combustor at altitude was much lower than that of the standard double-annular combustor with standard fuel nozzles at engine speeds below maximum. When the 3.0-gallon-per-hour nozzles were installed in the double-annular combustor at altitude (fig. 27(c)), however, the specific fuel consumption of the double-annular combustor with gasoline was as good as that of the single-annular combustor with JP-3 fuel. Installing the small nozzles in the double-annular combustor at 40,000 feet and a Mach number of 0.30 reduced the specific fuel consumption by as much as 35 percent, indicating a considerable potential gain in aircraft range by use of improved fuel nozzles.

Comparison of Basket Life

The double-annular combustor using gasoline showed no signs of warping or carbon deposit, whereas the single-annular combustor tended to warp longitudinally and the stiffeners had to be rewelded periodically (fig. 28(a)). After a running time of about 15 hours, the single-annular combustor using JP-3 showed a small carbon deposit near the fuel nozzles (fig. 28(b)), which did not become worse as running time increased. The basket was operated for approximately 108 hours. The designers have data (reference 5) which indicate that the pressure loss through the single-annular combustor can be reduced without appreciably affecting combustor performance.

CONCLUDING REMARKS

The most significant advantage of the single-annular combustor over the standard double-annular combustor was its improved combustion efficiency, as much as 17 to 30 percent at some conditions. However, this gain was not fully realized in the specific fuel consumption because of the large pressure loss through the single-annular combustor.

The turbine-discharge temperature profile of the double-annular combustor was more susceptible to inversion with increasing altitude than that of the single-annular combustor. Using smaller fuel nozzles at altitude, to simulate operation with duplex or variable-area type nozzles, essentially eliminated the tendency for inversion with the double-annular combustor. Ability to control the turbine-discharge temperature profile of the single-annular combustor by design techniques made it possible to operate at higher average tail-pipe temperatures without exceeding the manufacturer's recommended limit. Although fuel nozzle size had relatively little effect on the performance of the single-annular combustor, it had considerable effect on the performance of the double-annular combustor. Proper selection of fuel nozzles in the double-annular combustor using gasoline not only prevented temperature inversion but also provided specific fuel consumptions as low as values obtained with the single-annular combustor using JP-3.

The pressure loss through the single-annular combustor was approximately twice that of the double-annular combustor. At a given engine speed, no gains in thrust due to improved turbine temperature profile were realized because of this high pressure loss. However, the maximum thrust obtainable with the single-annular combustor was in some instances slightly greater than that of the double-annular combustor because of the ability of the single-annular combustor to operate at a higher average tail-pipe temperature without exceeding the turbine temperature limit.

At cruising and high speed engine operating conditions, the maximum operable altitude was essentially the same for both the single- and double-annular combustors. At altitudes below about 50,000 feet, the engine speed with the double-annular combustor could be reduced as much as 2200 rpm below the blow-out speed for the single-annular combustor.

Combustion efficiency and altitude operational limits with the single-annular combustor were essentially unaffected by changes in fuel volatility.

Lewis Flight Propulsion Laboratory
National Advisory Committee for Aeronautics
Cleveland, Ohio

APPENDIX - SYMBOLS AND CALCULATIONS

Symbols

A	area, sq ft
C_V	velocity coefficient, V/V'
F	thrust, lb
f	fuel-air ratio, $W_f/3600 W_a$
g	acceleration due to gravity, 32.2 ft/sec^2
H	enthalpy of air, Btu/lb
h_f	lower heating value of fuel, Btu/lb
N	engine speed, rpm
P	total pressure, lb/sq ft
p	static pressure, lb/sq ft
q	dynamic pressure, lb/sq ft
R	gas constant, $R_a = 53.34$, $R_g = 53.4$, ft-lb/(lb)($^{\circ}$ R)
T	total temperature, $^{\circ}$ R
t	static temperature, $^{\circ}$ R
V	velocity, ft/sec
W	weight flow, lb/sec
W_f	fuel flow, lb/hr
γ	ratio of specific heats
δ	ratio of compressor inlet total pressure to standard sea-level pressure of 2116 lb/sq ft
η_b	combustion efficiency, percent
θ	ratio of compressor inlet total temperature to standard sea-level temperature of 519° R

λ a term accounting for difference between enthalpy of carbon dioxide and water vapor in burned mixture and enthalpy of oxygen removed from air by their formation

ρ density, lb/cu ft

Subscripts:

a air

g gas

i indicated

j jet

n net

t exhaust-nozzle throat

0 free-stream conditions

Numbered subscripts refer to instrumentation stations within the engine (fig. 3).

Prime superscripts refer to calculations assuming an isentropic process.

Methods of Calculation

Temperature. - The total temperature was determined by a calibration of the types of thermocouple used. This calibration resulted in a tabulation of T_1/T against p/P .

Air flow. - Air flow was determined from the measurements of temperature and pressure at station 1 as follows:

$$W_{a,1} = \frac{P_1 A_1}{T_1} \sqrt{\frac{2gr T_1}{R(\gamma-1)} \left[\left(\frac{P_1}{P_1}\right)^{\frac{2}{\gamma}} - \left(\frac{P_1}{P_1}\right)^{\frac{\gamma+1}{\gamma}} \right]} \quad (1)$$

where

$$\gamma = 1.4$$

Jet thrust. - The jet thrust was determined from the equation

$$F_j = \frac{W_{g,6} C_V V_t'}{g} + A_7 (P_t - P_0)$$

where a velocity coefficient C_V of 0.98 was assumed.

Net thrust. - The net thrust was determined by subtracting the inlet momentum of the air, at the particular simulated flight speed, from the jet thrust. Thus

$$F_n = F_j - \frac{W_{a,1} V_0}{g}$$

Combustion efficiency. - The combustion efficiency was computed from the following equation:

$$\eta_b = \frac{H_{a,4} - H_{a,3} + f\lambda_4}{f h_f}$$

where the base temperature for λ is 540° R (reference 6).

Combustor pressure loss. - The combustor pressure loss was defined as

$$\frac{P_3 - P_4}{q_3}$$

where

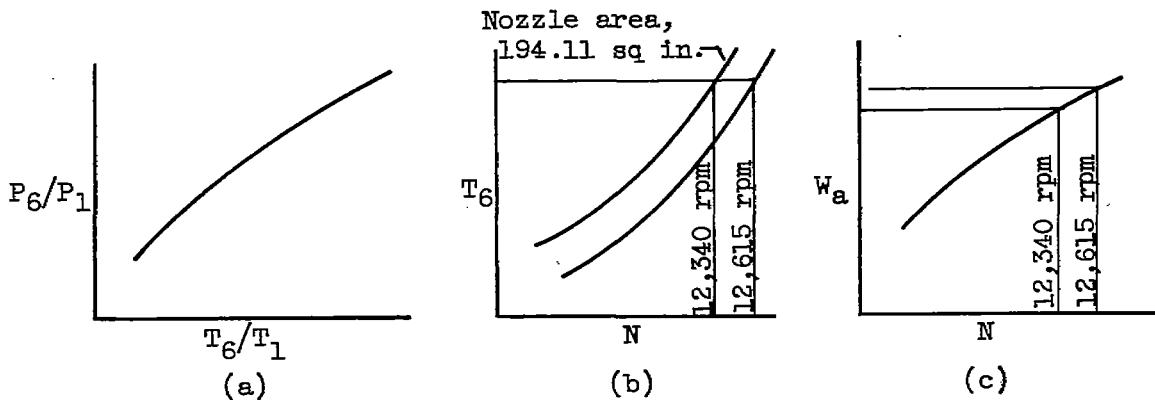
$$q_3 = \frac{\rho_3 V_3^2}{2g}$$

Method of data adjustment. - The exhaust-nozzle area of the engine with the double-annular combustor and 7.0-gallon-per-hour fuel nozzles was sized so that the turbine temperature limit occurred at rated speed (12,500 rpm) at an altitude of 5000 feet and a flight Mach number of 0. At an altitude of 20,000 feet and a flight Mach number of 0.60, limiting temperature occurred at 12,615 rpm.

With the installation of the single-annular combustor, the exhaust nozzle had to be resized because of the higher pressure loss of this combustor. Because of structural limitations of the single-annular combustor, which necessitated operation at only the higher altitudes, the nozzle area could not be sized in the same manner as for the double-annular combustor. The nozzle area was estimated at 194.1 square inches

which later proved to be slightly in error. In order to make the data for the two combustors directly comparable, the data for the single-annular combustor were adjusted to values which would have been obtained had the exhaust-nozzle area been such that limiting temperature would have been reached at an engine speed of 12,615 rpm using the 10.5-gallon-per-hour fuel nozzles and operating at an altitude of 20,000 feet and a Mach number of 0.60.

Adjustment of the data made use of the principle of engine pumping characteristics described in reference 7. A plot of engine pressure ratio against engine temperature ratio would be similar to sketch (a). For a given flight condition, the tail-pipe pressure would be a function



of only the tail-pipe temperature. If the tail-pipe temperature is maintained constant, a change in exhaust-nozzle area, and consequently engine speed, will not change the tail-pipe pressure, provided the change is small enough that component efficiencies through the engine remain essentially constant.

With the single-annular combustor, 10.5-gallon-per-hour fuel nozzles, flight Mach number of 0.60, altitude of 20,000 feet, and exhaust-nozzle area of 194.1 square inches, the engine speed at limiting temperature was 12,340 rpm, as indicated by sketch (b). At constant tail-pipe temperature, the engine speed was adjusted to 12,615 rpm, which was the temperature-limited speed with the double-annular combustor at the same flight conditions. Then, from a plot of air flow against engine speed (sketch (c)), the increase in air flow, due to the increase in engine speed, was determined. The increase in air flow proved to be exactly 1.0 percent. Because the tail-pipe pressure and temperature remained constant, the increase in nozzle area necessary to pass the increased air flow was also 1.0 percent, the new area being 196.0 square inches.

Net thrust is defined by the equation

$$F_n = W_a \left[\frac{V_7}{g} (1+f) - \frac{V_0}{g} \right]$$

Changing the exhaust-nozzle area a small amount while maintaining a constant average tail-pipe temperature will not affect V_7 (T_7 and P_7 will remain constant) or V_0 . The fuel-air ratio will remain constant unless there is a change in combustion efficiency. In reference 8, it is indicated that for an area change of 1.00 percent, the change in combustion efficiency will be insignificant. Any change in net thrust will therefore be a function of only the change in air flow.

$$\left(\frac{F_n}{\delta} \right)_{\text{adjusted}} = \left(\frac{F_n}{\delta} \right)_{\text{unadjusted}} \frac{\left(\frac{W_a \sqrt{\theta}}{\delta} \right)_{\text{adjusted}}}{\left(\frac{W_a \sqrt{\theta}}{\delta} \right)_{\text{unadjusted}}}$$

The thrusts and air flows for the single-annular combustor were adjusted by multiplying by 1.010. The adjusted engine speeds were determined for the corresponding adjusted air flows by means of plots similar to sketch (c).

REFERENCES

1. Straight, David M., and Gold, Harold: Experimental and Analytical Study of Balanced-Diaphragm Fuel Distributors for Gas-Turbine Engines. NACA RM E50F05, 1950.
2. Zettle, Eugene V., and Mark, Herman: Simulated Altitude Performance of Two Annular Combustors with Continuous Axial Openings for Admission of Primary Air. NACA RM E50E18a, 1950.
3. Dowman, Harry W., and Younger, George G.: Comparison of Performance of AN-F-28 Fuel and Gasoline in J34-WE-22 Turbojet Engine. NACA RM E8L10a, 1949.
4. Childs, J. Howard, McCafferty, Richard J., and Surine, Oakley, W.: Effect of Combustor-Inlet Conditions on Performance of an Annular Turbojet Combustor. NACA Rep. 881, 1947. (Formerly NACA TN 1357.)
5. Mark, Herman, and Zettle, Eugene V.: Effect of Air Distribution on Radial Temperature Distribution in One-Sixth Sector of Annular Turbojet Combustor. NACA RM E9I22, 1950.

- 2397
6. Turner, L. Richard, Addie, Albert N., and Zimmerman, Richard H.: Charts for the Analysis of One-Dimensional Steady Compressible Flow. NACA TN 1419, 1948.
 7. Sanders, Newell D., and Behun, Michael: Generalization of Turbojet-Engine Performance in Terms of Pumping Characteristics. NACA TN 1927, 1949.
 8. Campbell, Carl E.: Altitude-Wind-Tunnel Investigation of a 3000-Pound-Thrust Axial-Flow Turbojet Engine. III - Analysis of Combustion-Chamber Performance. NACA RM E8B19, 1948.

TABLE I - FUEL ANALYSIS



Fuel	MIL-F-5572 (clear gasoline)	MIL-F-5624A (JP-3)	Low volatility fuel
Distillation			
Initial boiling point, °F	118	105	181
Percentage evaporated			
5	140	-----	242
10	157	154	271
20	178	196	300
30	198	240	319
40	213	283	332
50	226	326	351
60	240	359	365
70	252	388	381
80	267	420	403
90	290	472	441
95	308	-----	470
Final boiling point, °F	344	558	508
Residue, percent	-----	-----	1.0
Loss, percent	-----	-----	0.5
Reid vapor pressure, lb/sq in.	6.6	7.0	1.0
Specific gravity at 60° F/60° F	0.720	0.757	0.780
Hydrogen-carbon ratio	0.179	0.171	0.170
Net heat, Btu/lb by aniline point correlation	18,860	18,760	18,691
Refraction index, -20° C	1.4043	1.4217	1.4329
Aniline point, °C	57.3	-----	62.1
Freezing point, °C	-----	-----	below-60
Silica gel aromatics, volume percent	-----	-----	5.72
Bromine number	-----	-----	1.4
Olefins, percent	-----	-----	1.3
Air jet gum, mg/100 ml	-----	-----	2
Accelerated air jet gum, mg/100 ml	-----	-----	5

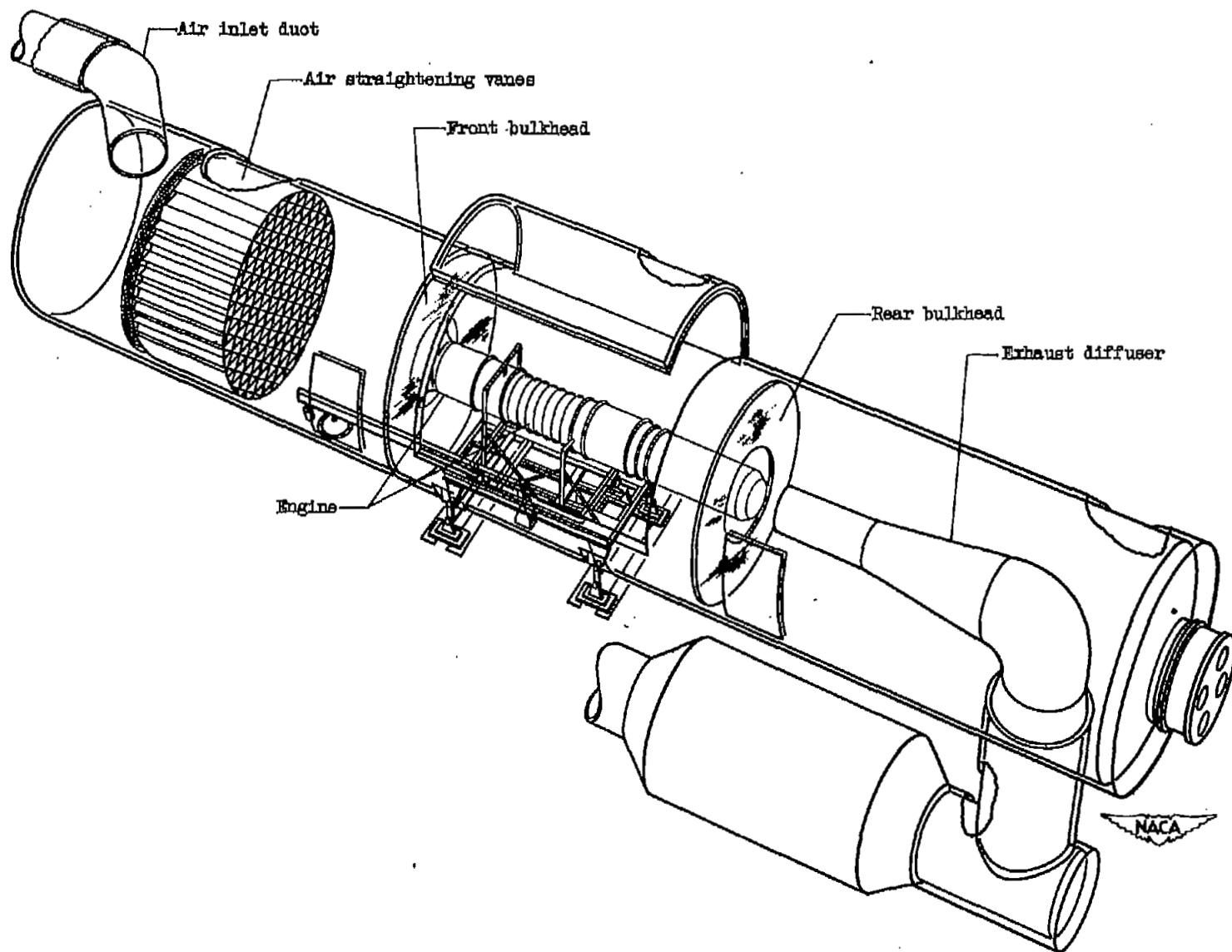


Figure 1. - Schematic diagram of altitude-test chamber.

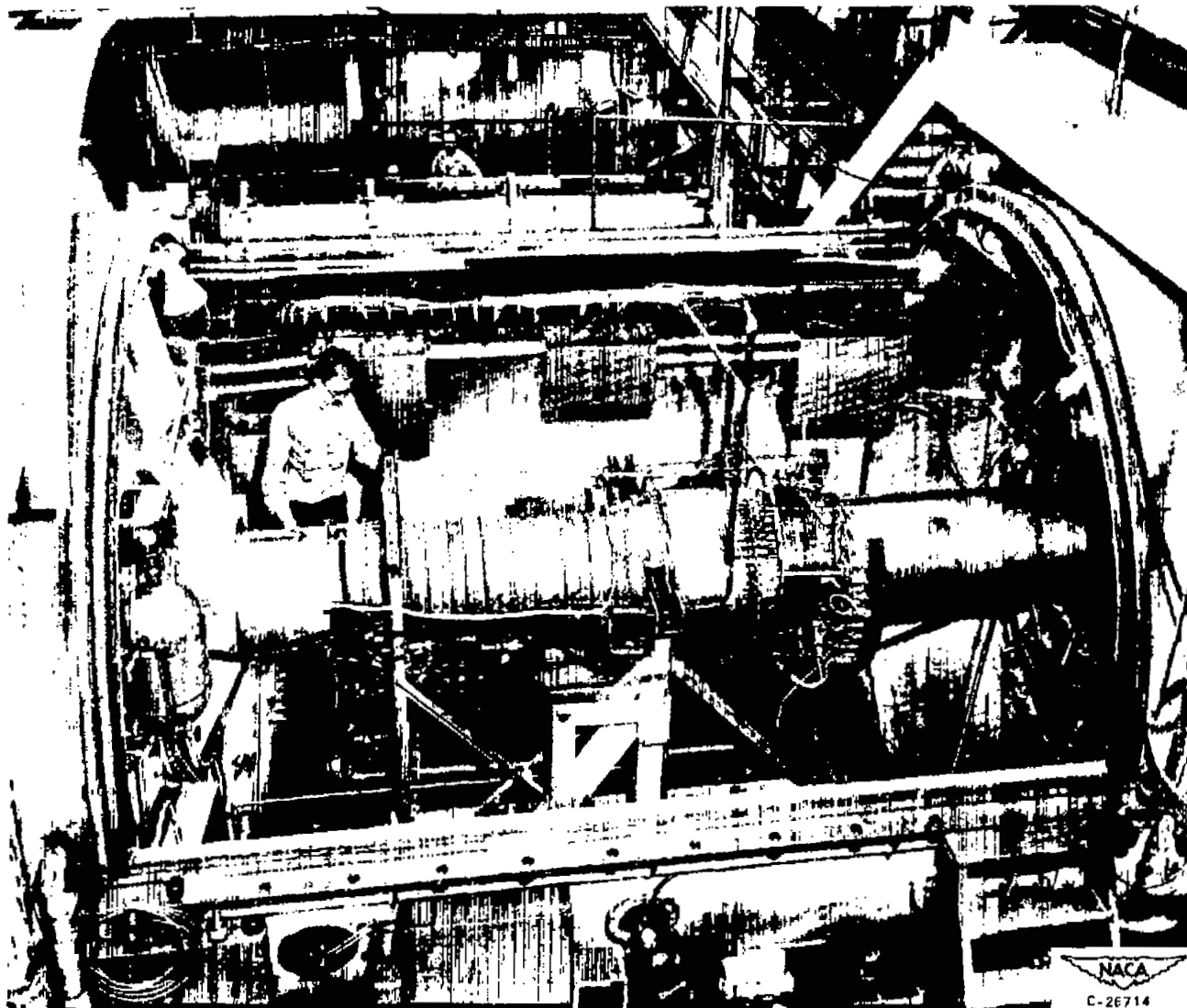


Figure 2. - J34-WE-18 turbojet engine installed in test section.

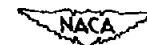
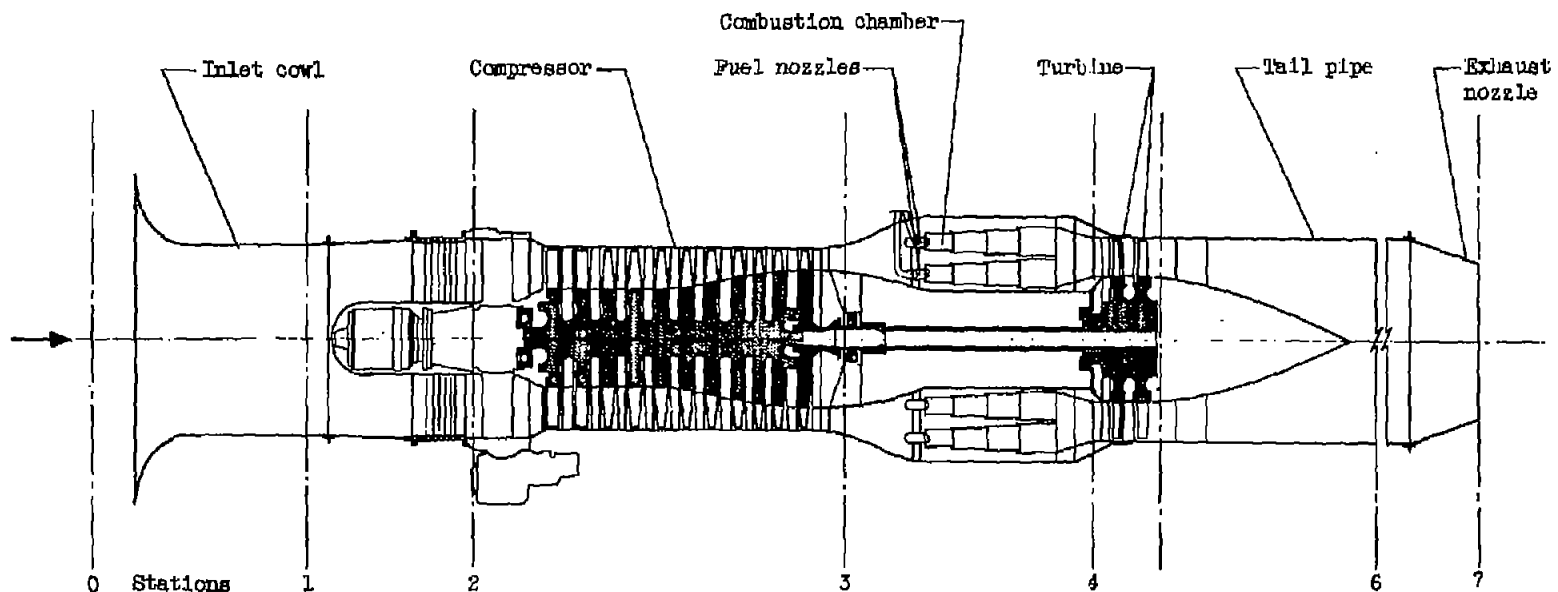
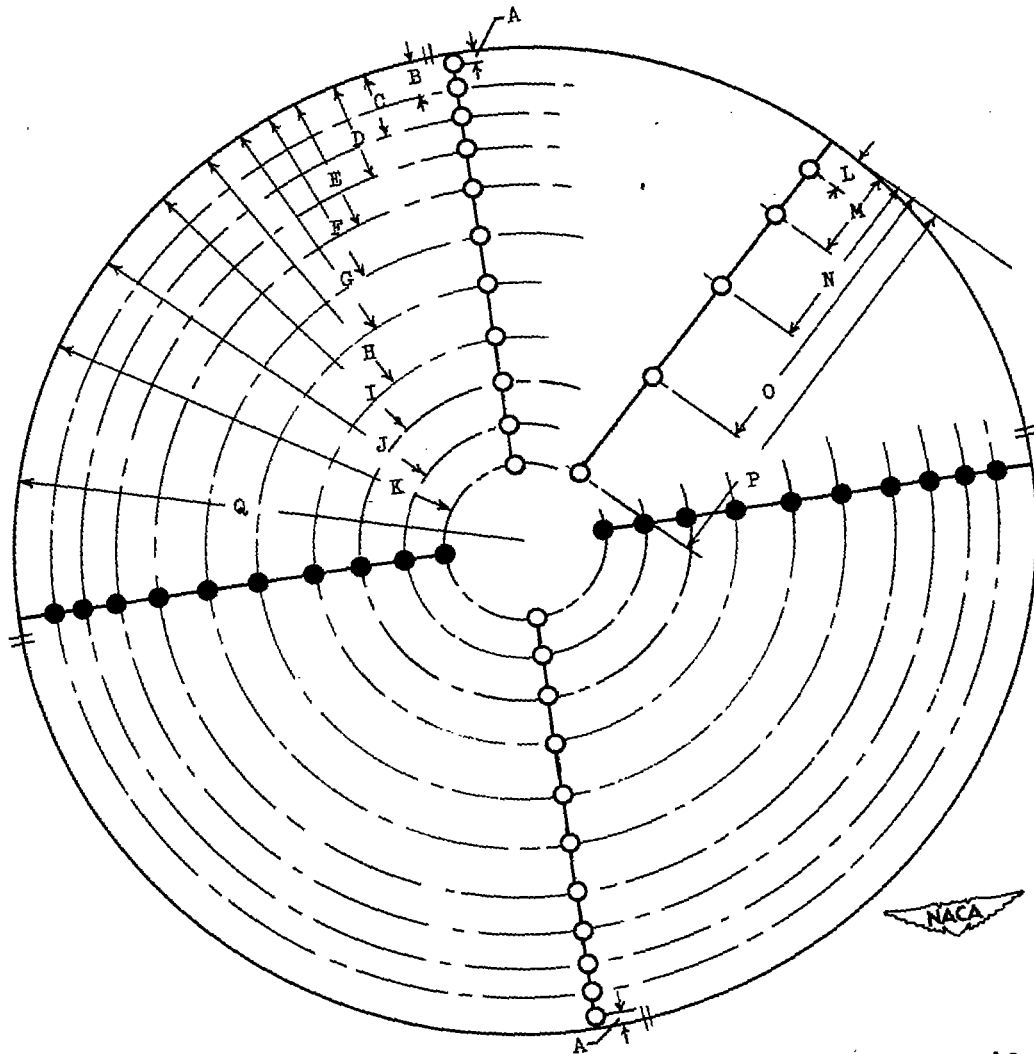


Figure 3. - Sectional view of engine showing instrumentation stations.



A = 0.059 in.
 B = .279
 C = .839
 D = 1.409
 E = 2.049
 F = 2.729
 G = 3.469
 H = 4.299
 I = 5.261

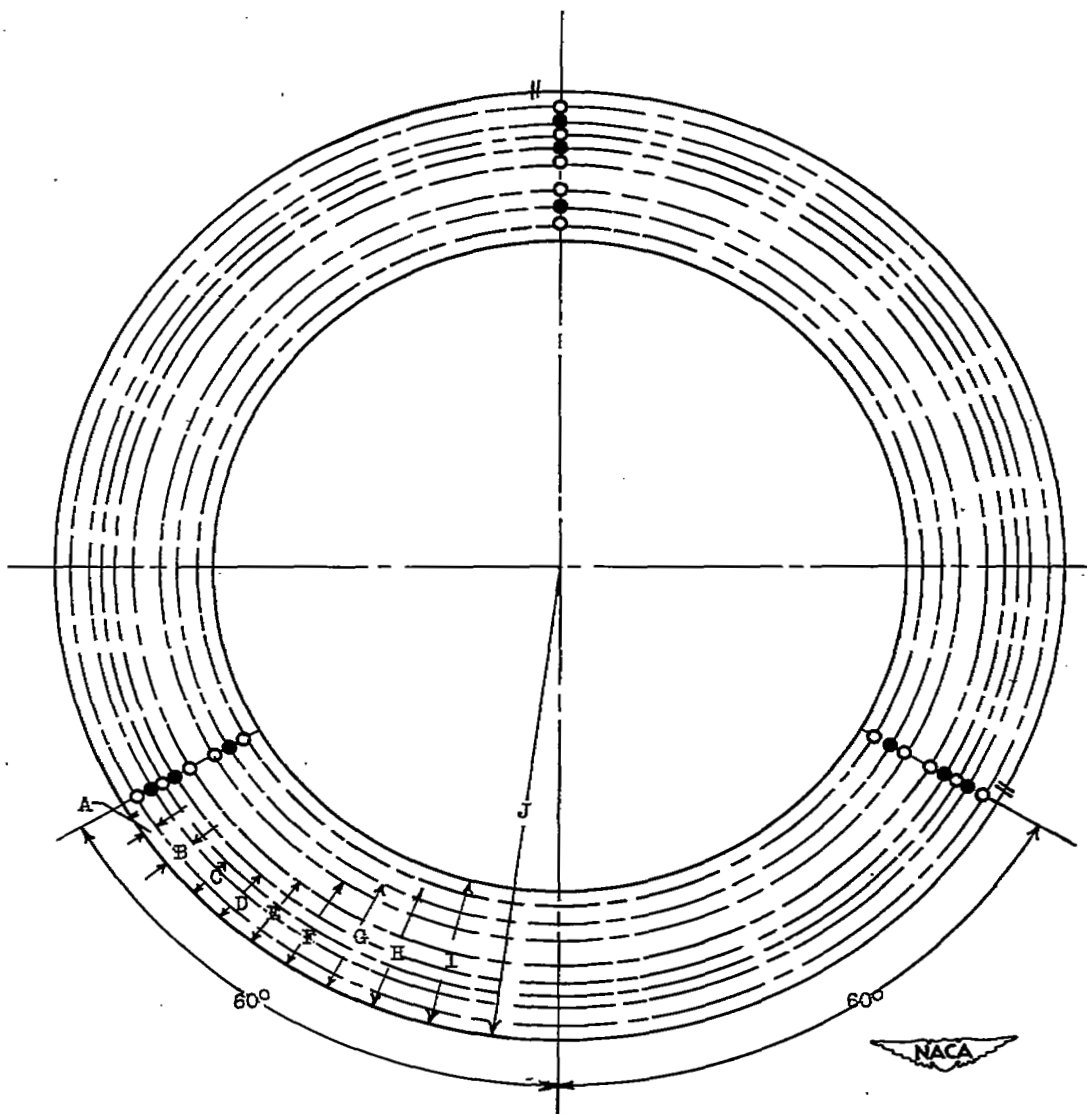
J = 6.439 in.
 K = 8.159
 L = .839
 M = 2.049
 N = 3.469
 O = 5.279
 P = 8.159
 Q = 10.50

- Total-pressure probe
- Total-temperature probe
- Stream static probe
- || Wall static probe

(a) Station 1, engine inlet.

Figure 4. - Engine instrumentation.

2397



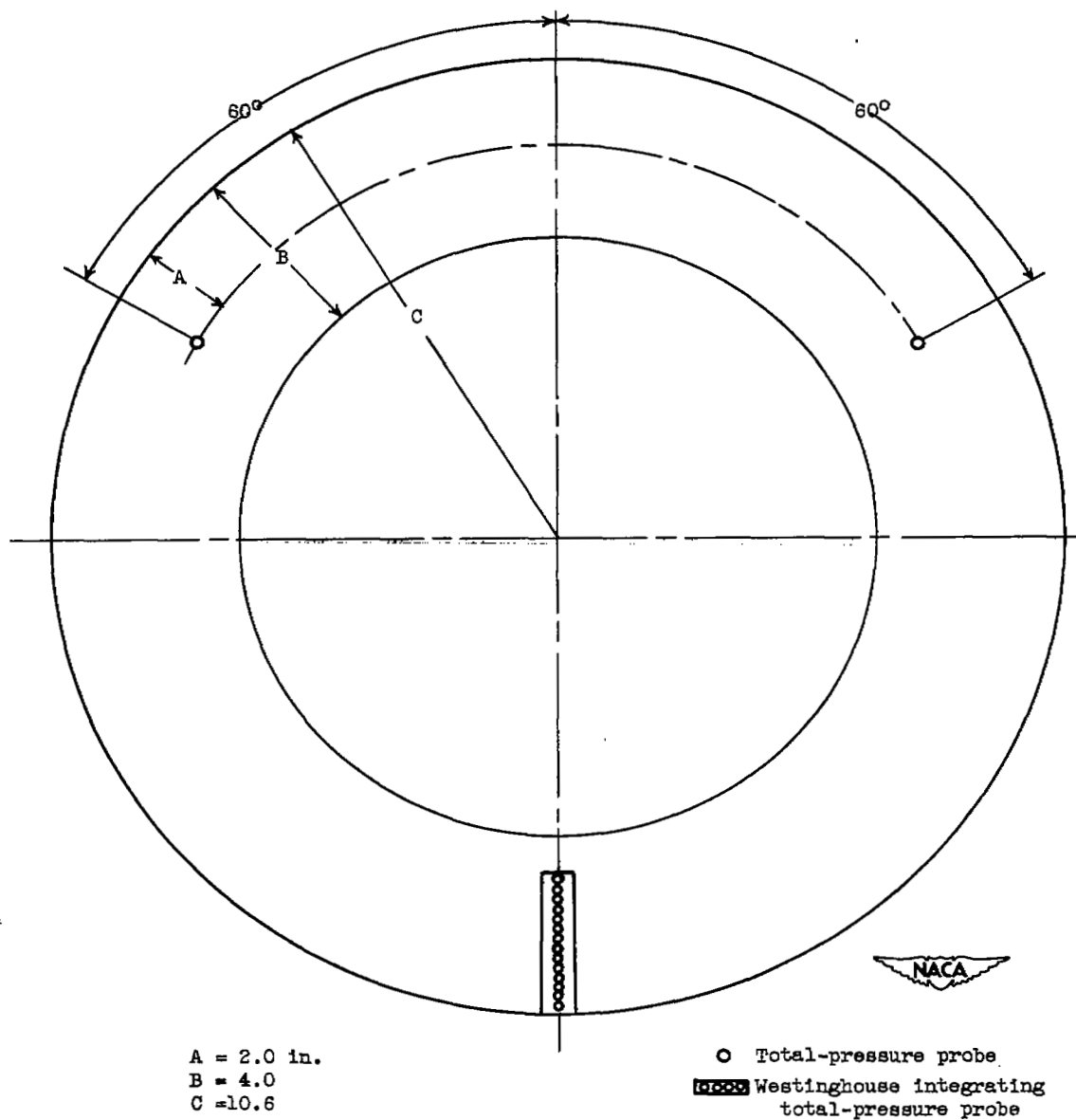
A = 0.278 in.
 B = .558
 C = .838
 D = 1.138
 E = 1.438

F = 2.038 in.
 G = 2.388
 H = 2.738
 I = 3.100
 J = 9.890

○ Total-pressure probe
 ● Total-temperature probe
 | Wall static probe

(b) Station 3, compressor outlet.

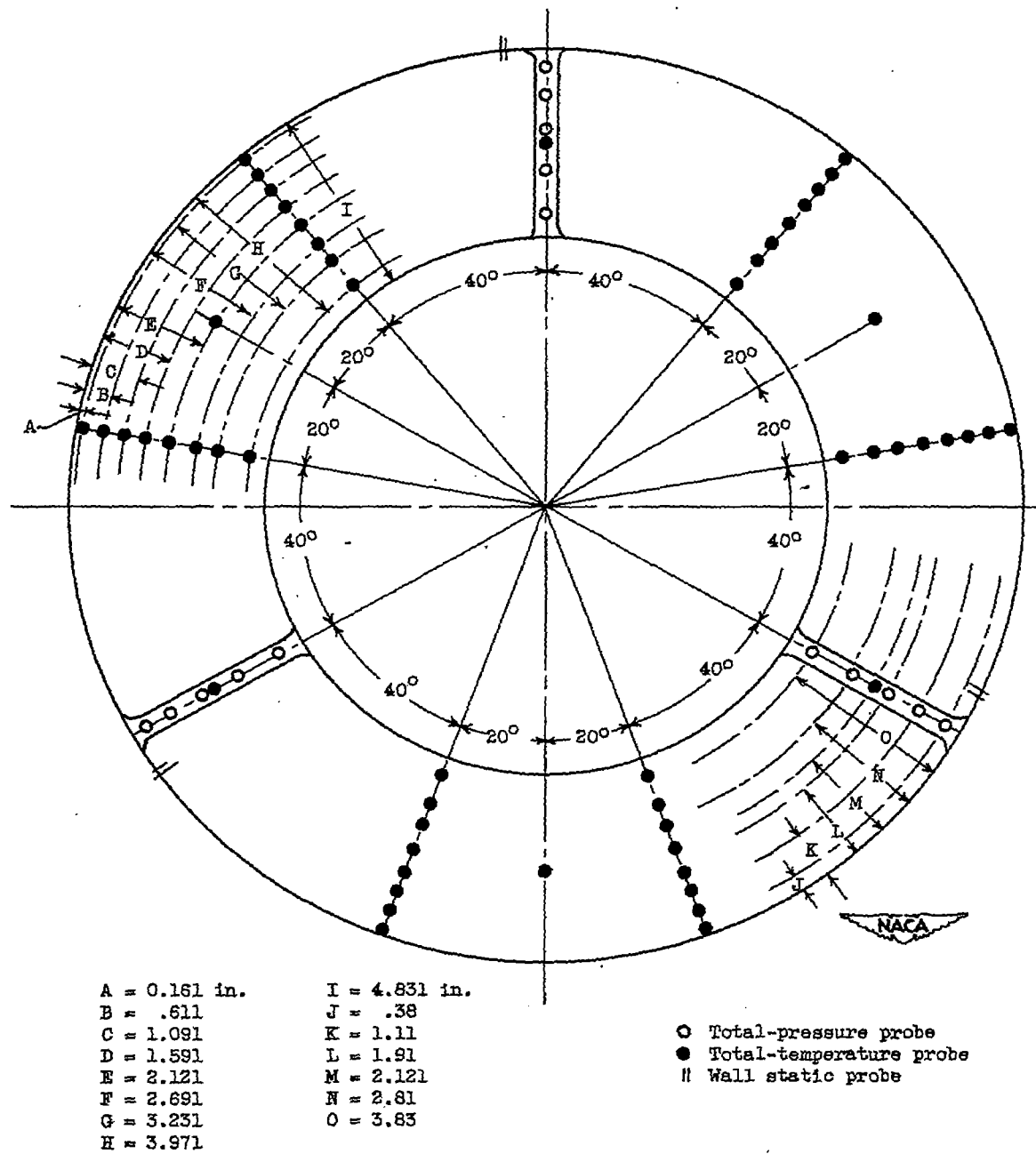
Figure 4. - Continued. Engine instrumentation.



(c) Station 4, turbine inlet.

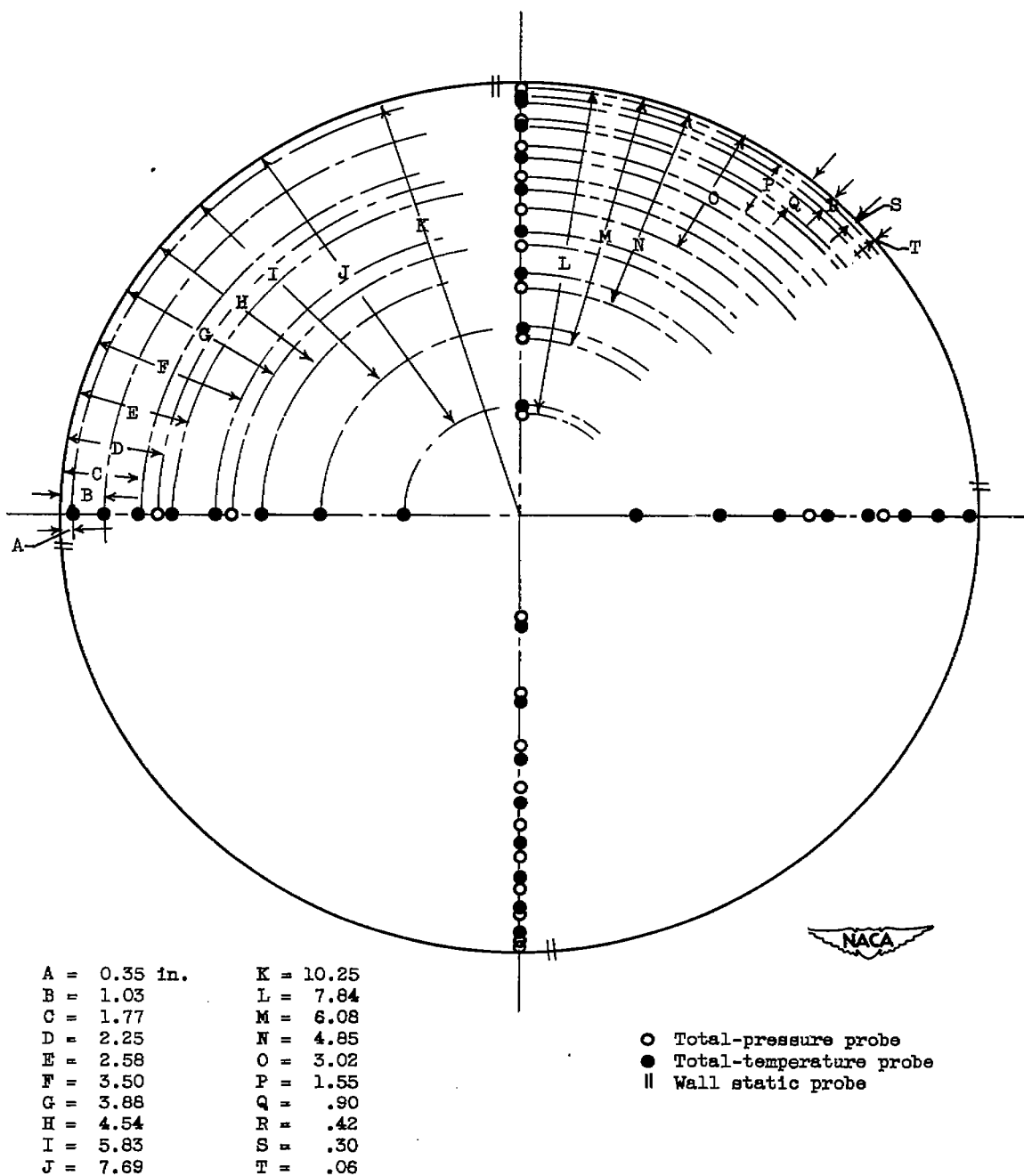
Figure 4. - Continued. Engine instrumentation.

1637



(d) Station 5, turbine outlet.

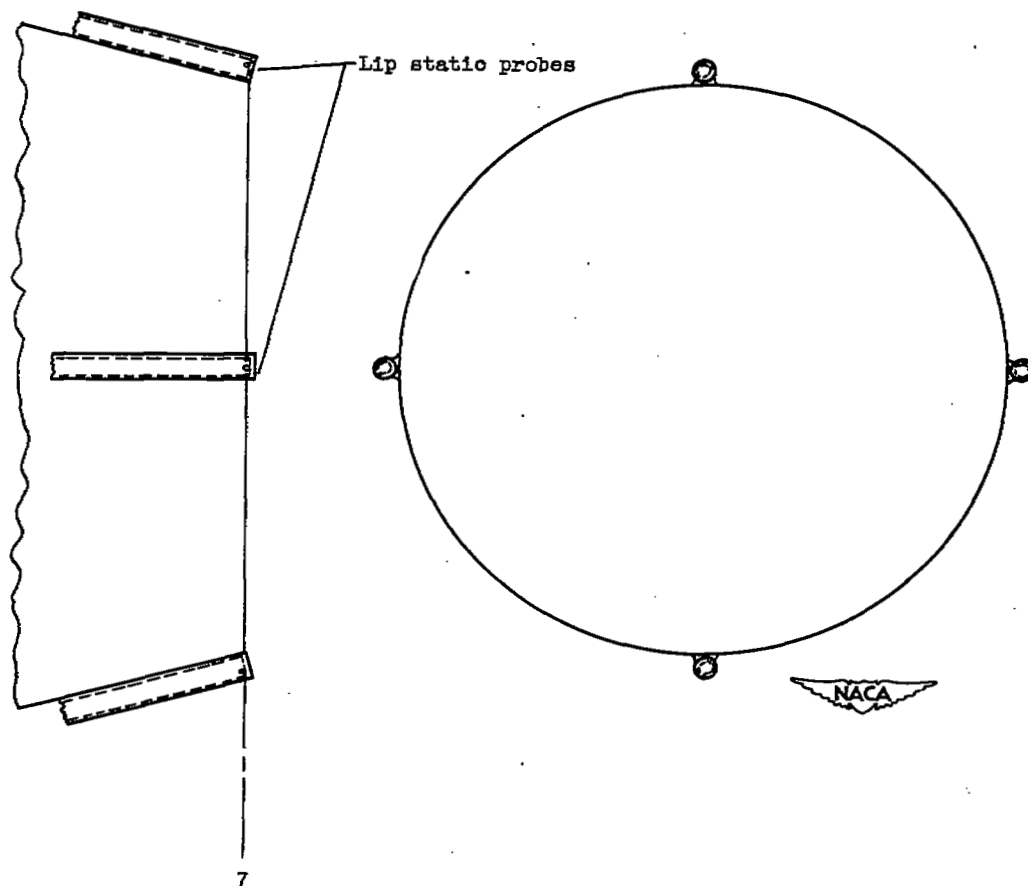
Figure 4. - Continued. Engine instrumentation.



(e) Station 6, exhaust-nozzle inlet.

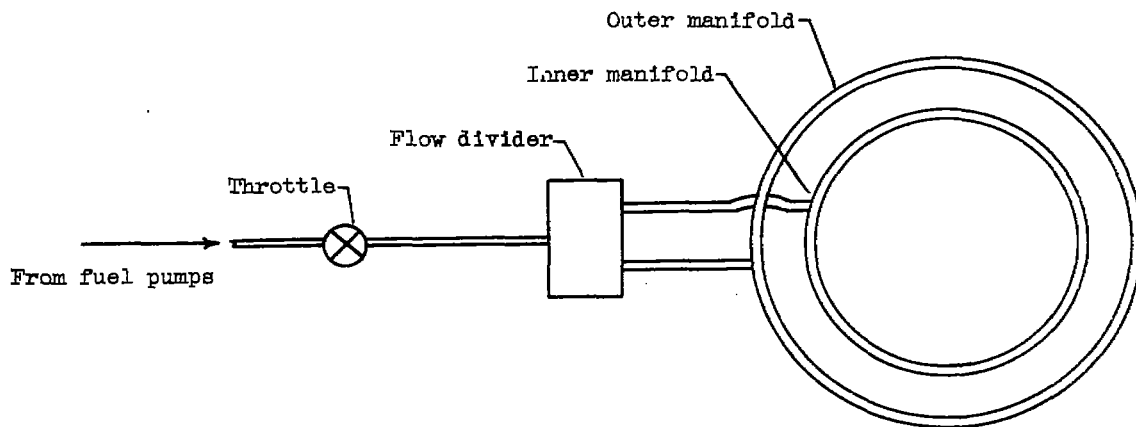
Figure 4. - Continued. Engine instrumentation.

2391

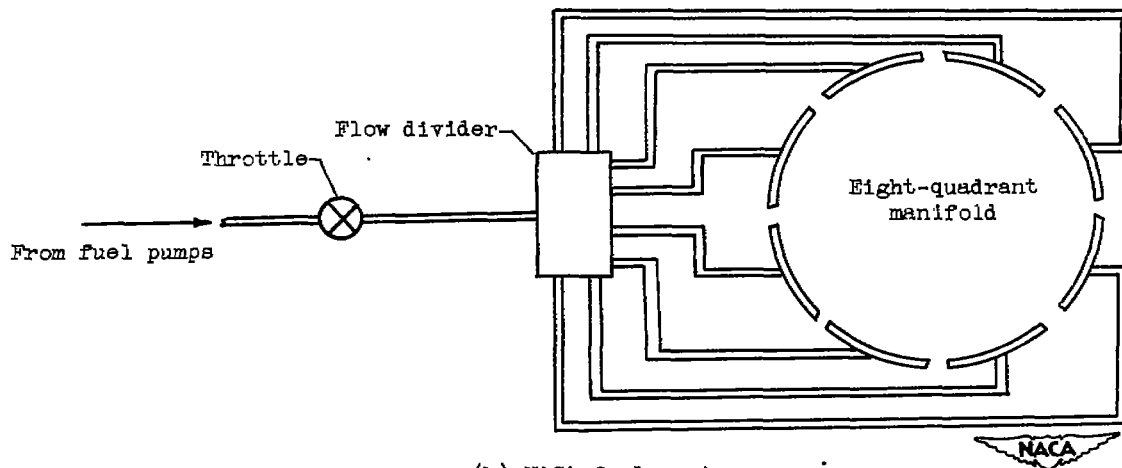


(f) Station 7, exhaust-nozzle exit.

Figure 4. - Concluded. Engine instrumentation.



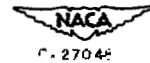
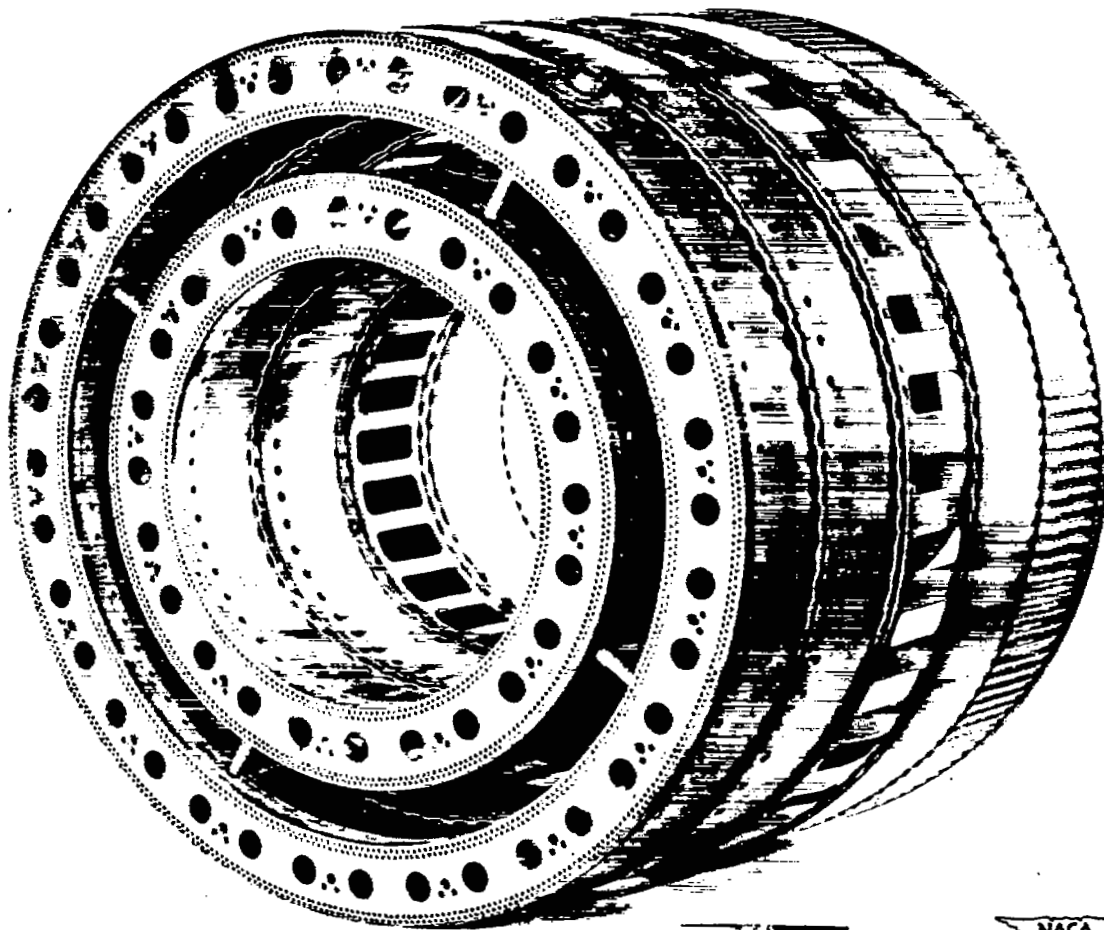
(a) Standard fuel system.



(b) NACA fuel system.

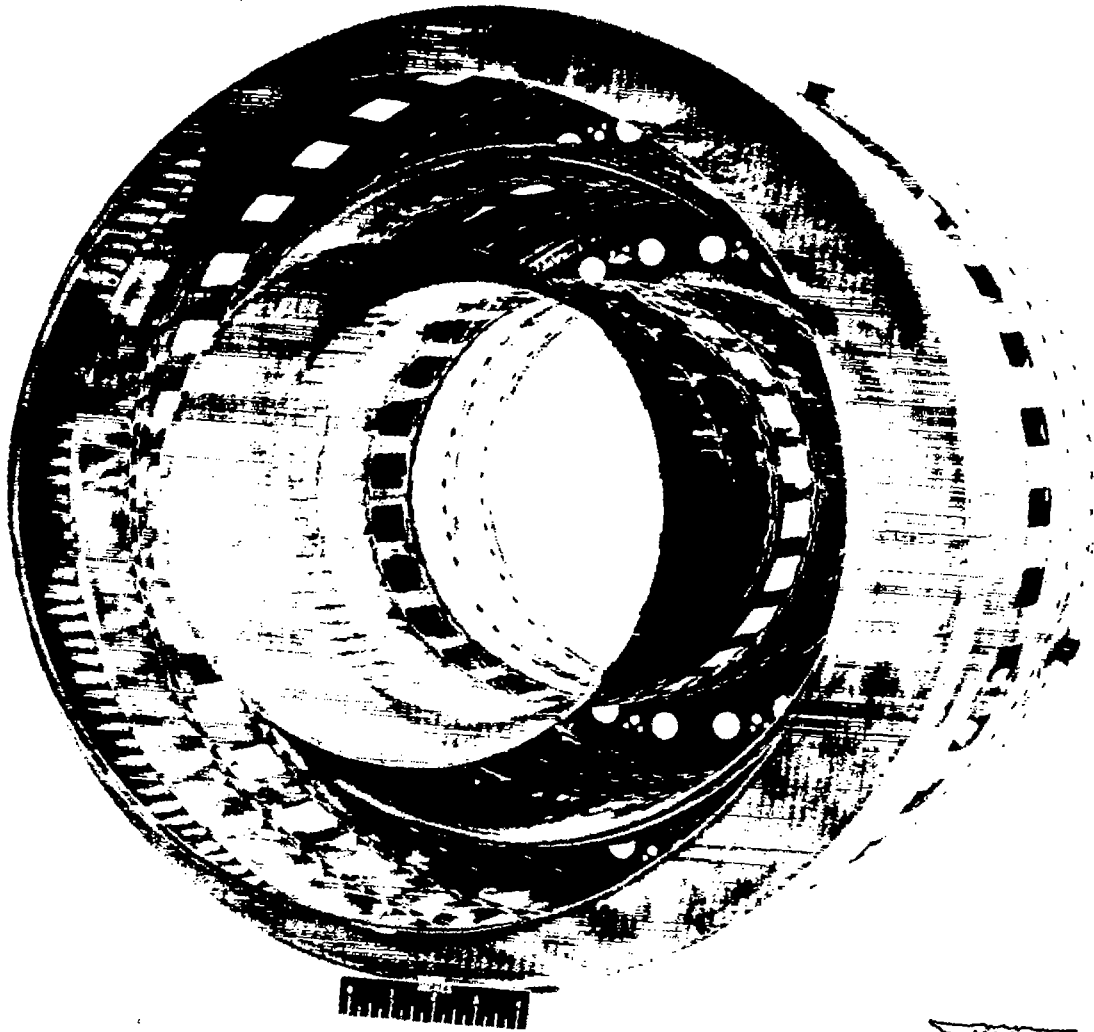
Figure 5. - Schematic diagram of engine fuel systems.

2397



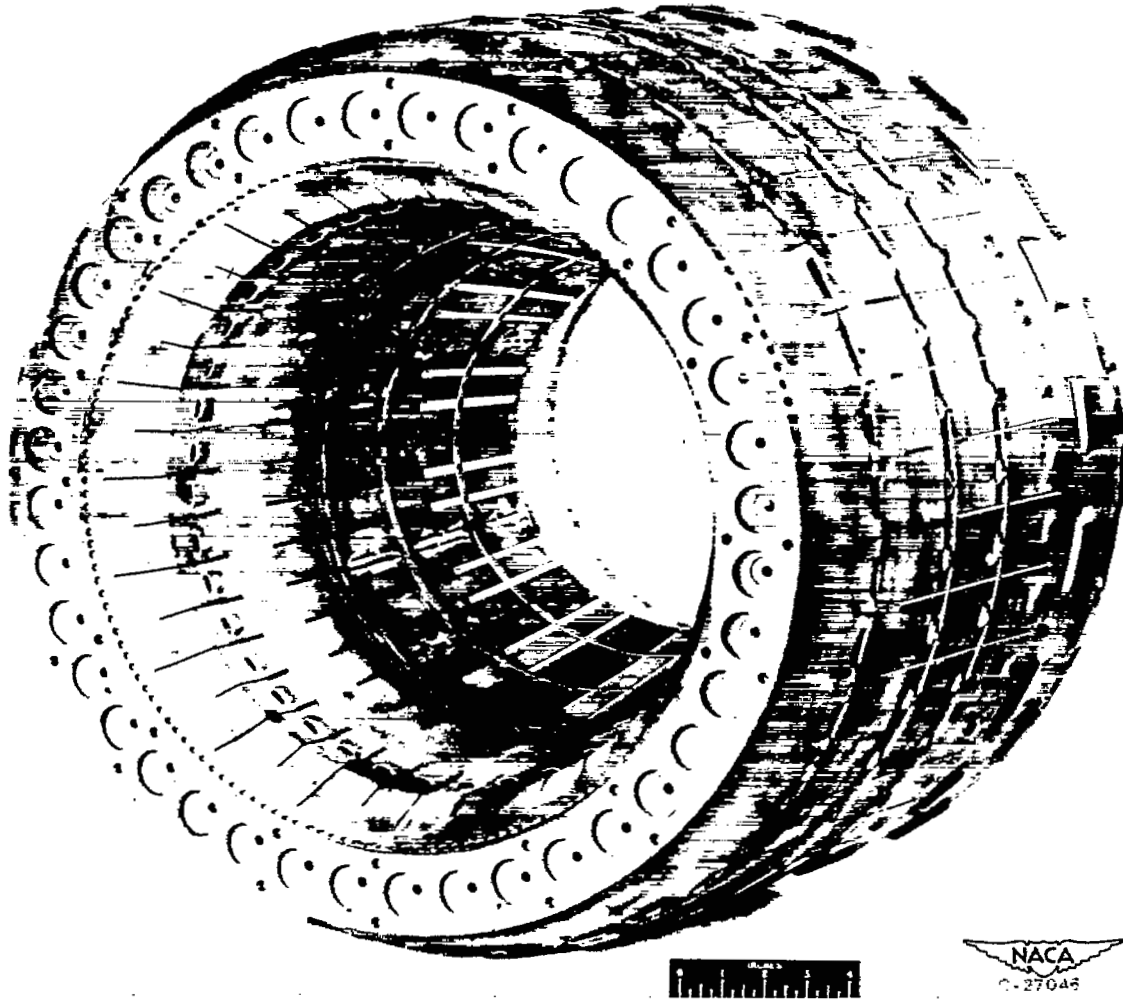
(a) Combustor-inlet quarter view.

Figure 6. - Standard combustor of turbojet engine.



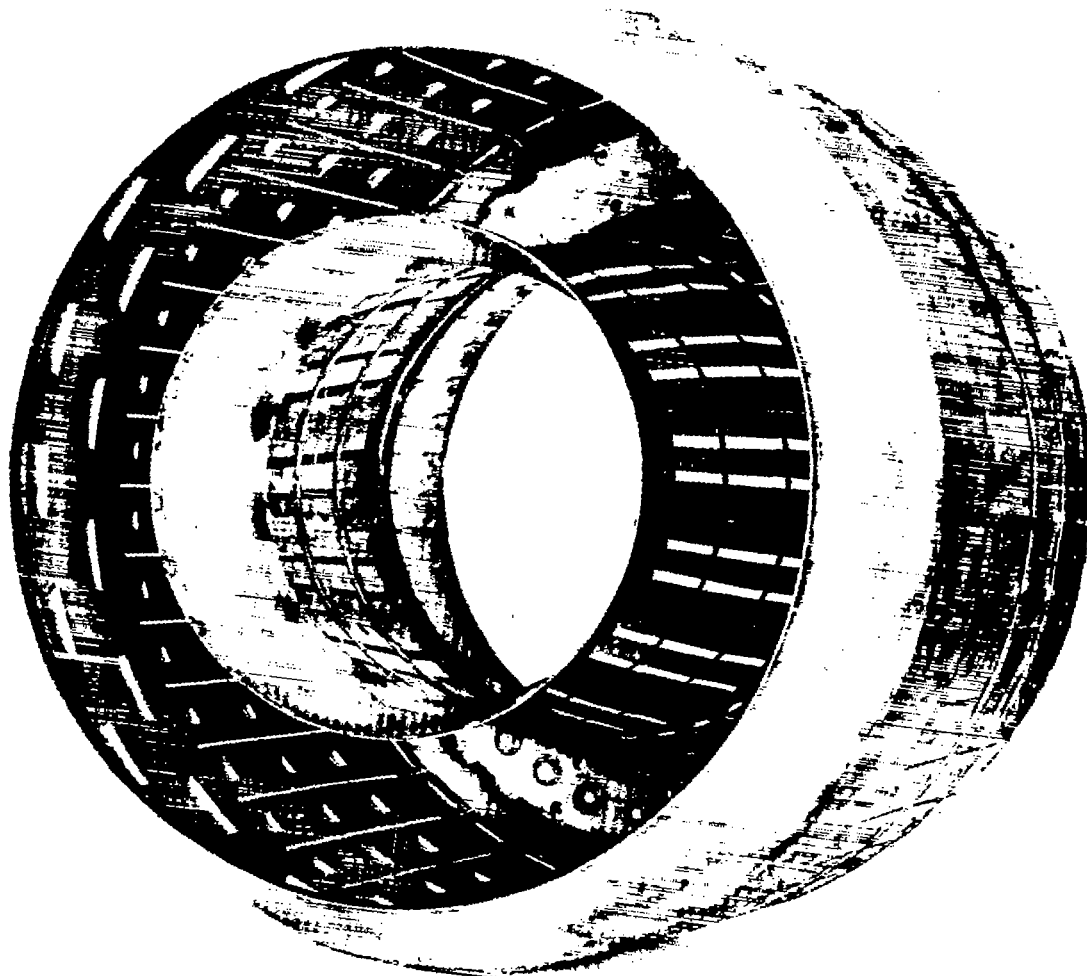
(b) Combustor-outlet quarter view.

Figure 6. - Concluded. Standard combustor of turbojet engine.



(a) Combustor-inlet quarter view.

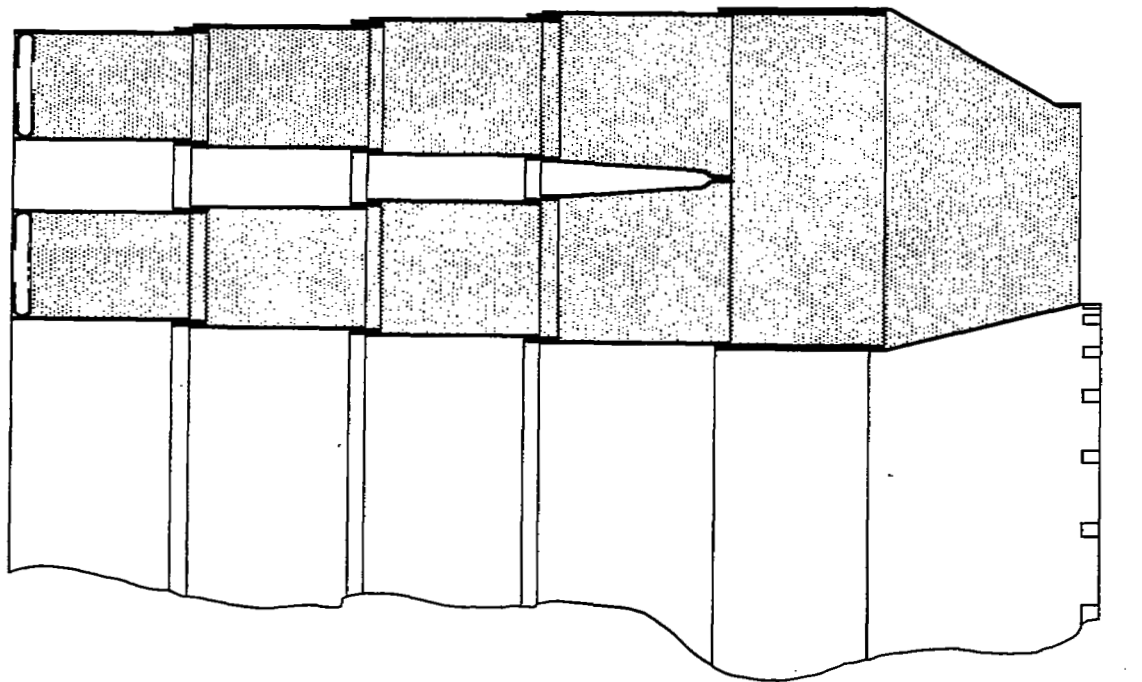
Figure 7. - NACA combustor model 1.



(b) Combustor-outlet quarter view.
Figure 7. - Concluded. NACA combustor model 1.

NACA
C-27047

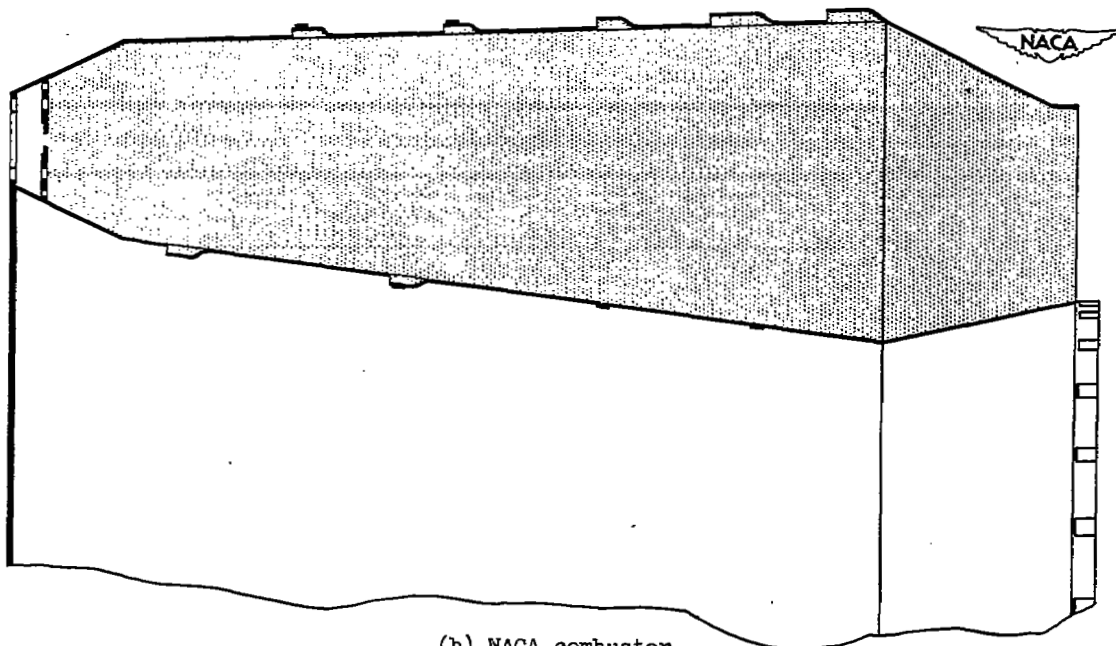
2397



(a) Standard combustor.

Combustion zone

Air flow →



(b) NACA combustor.

Figure 8. - Comparison of standard combustor and NACA combustor cross sections.

24 32

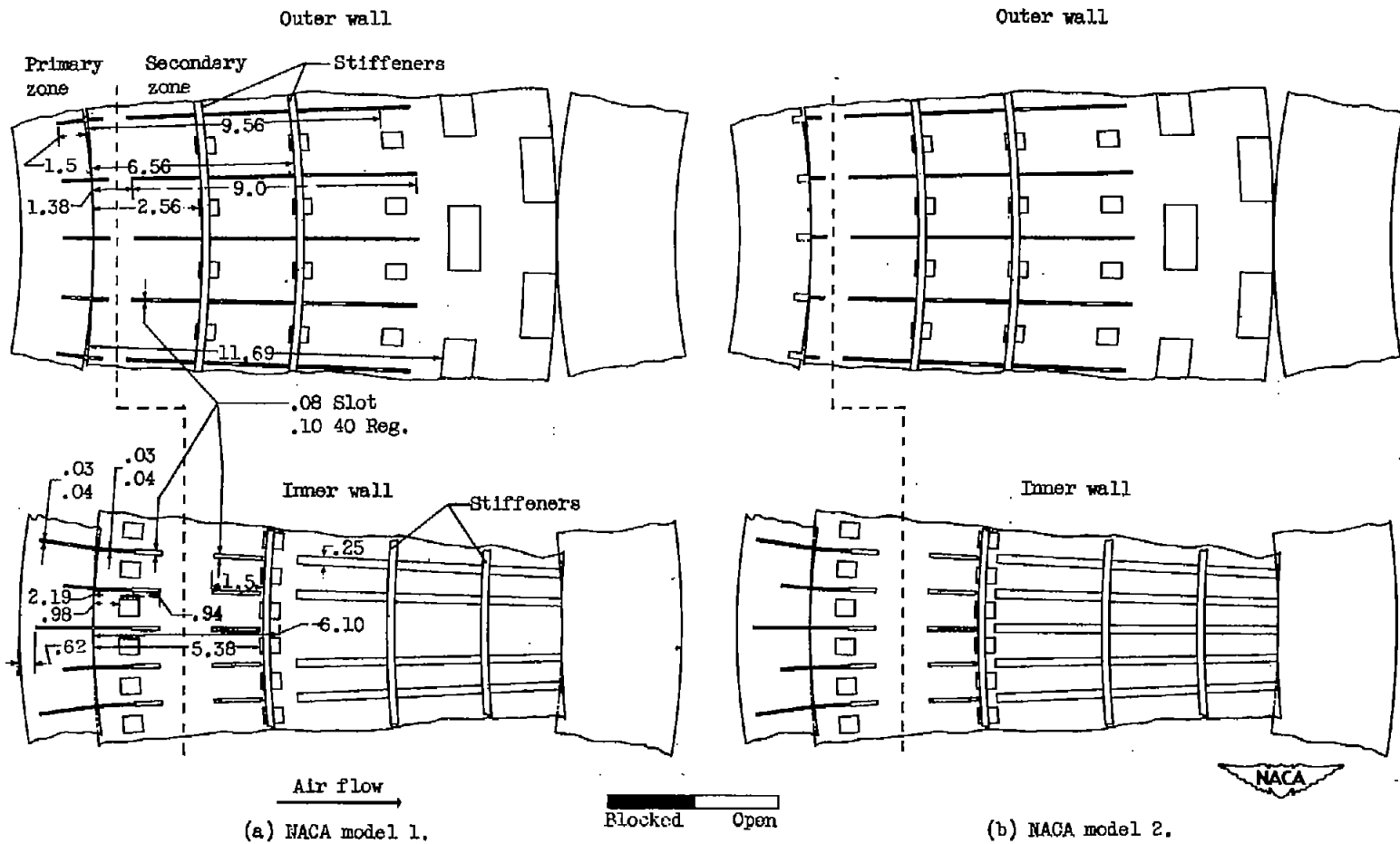


Figure 9. - Detailed drawings of NACA combustor models.

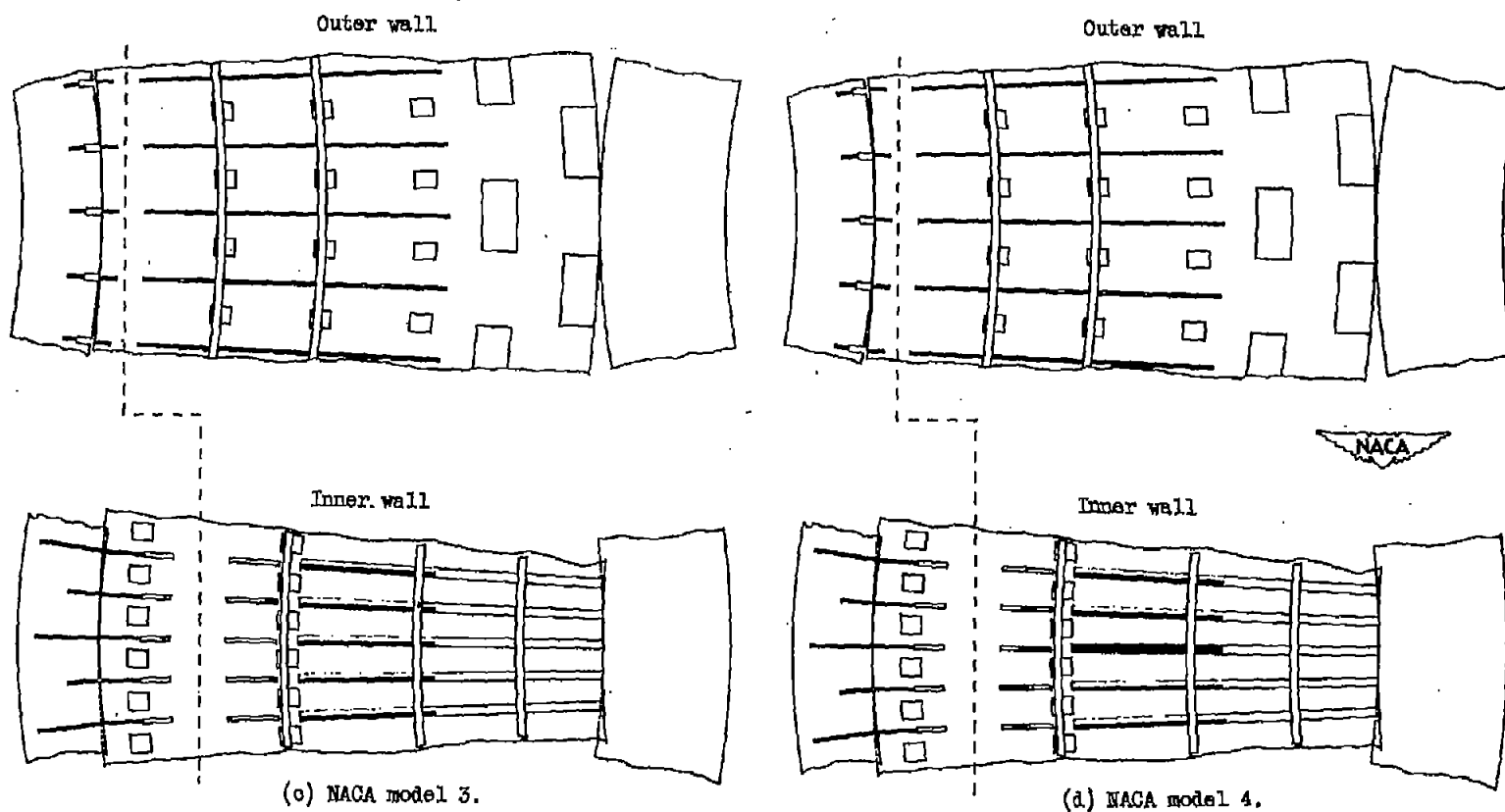


Figure 9. - Continued. Detailed drawings of NACA combustor models.

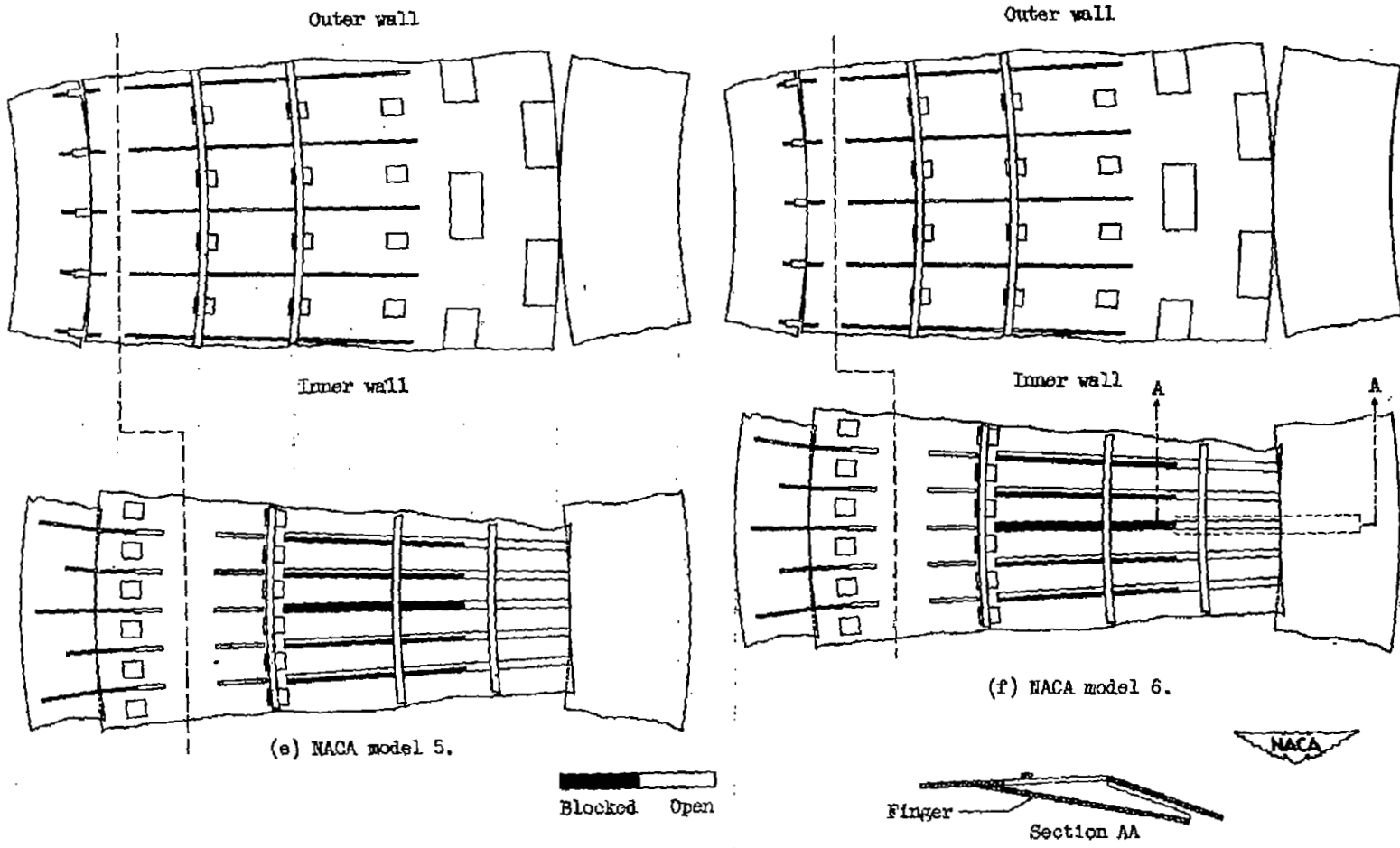
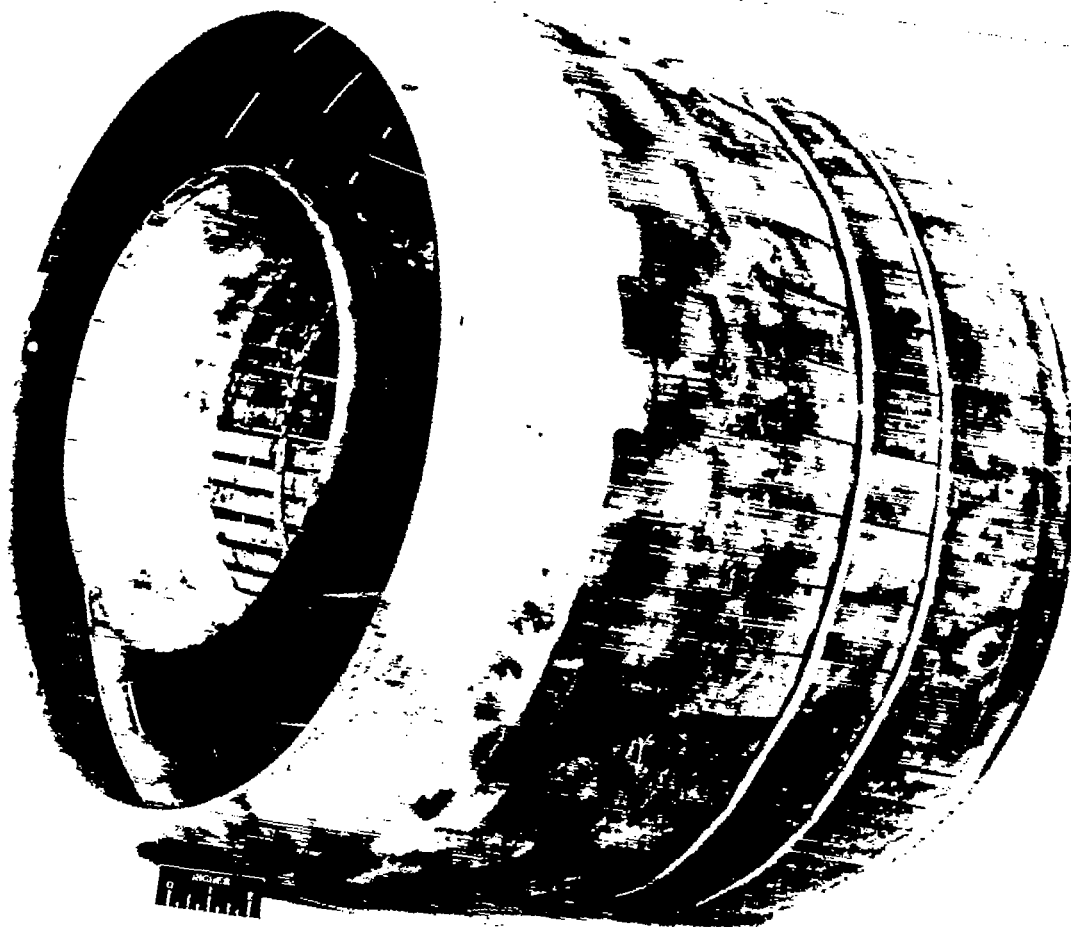


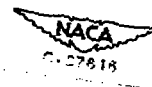
Figure 9. - Concluded. Detailed drawings of NACA combustor models.

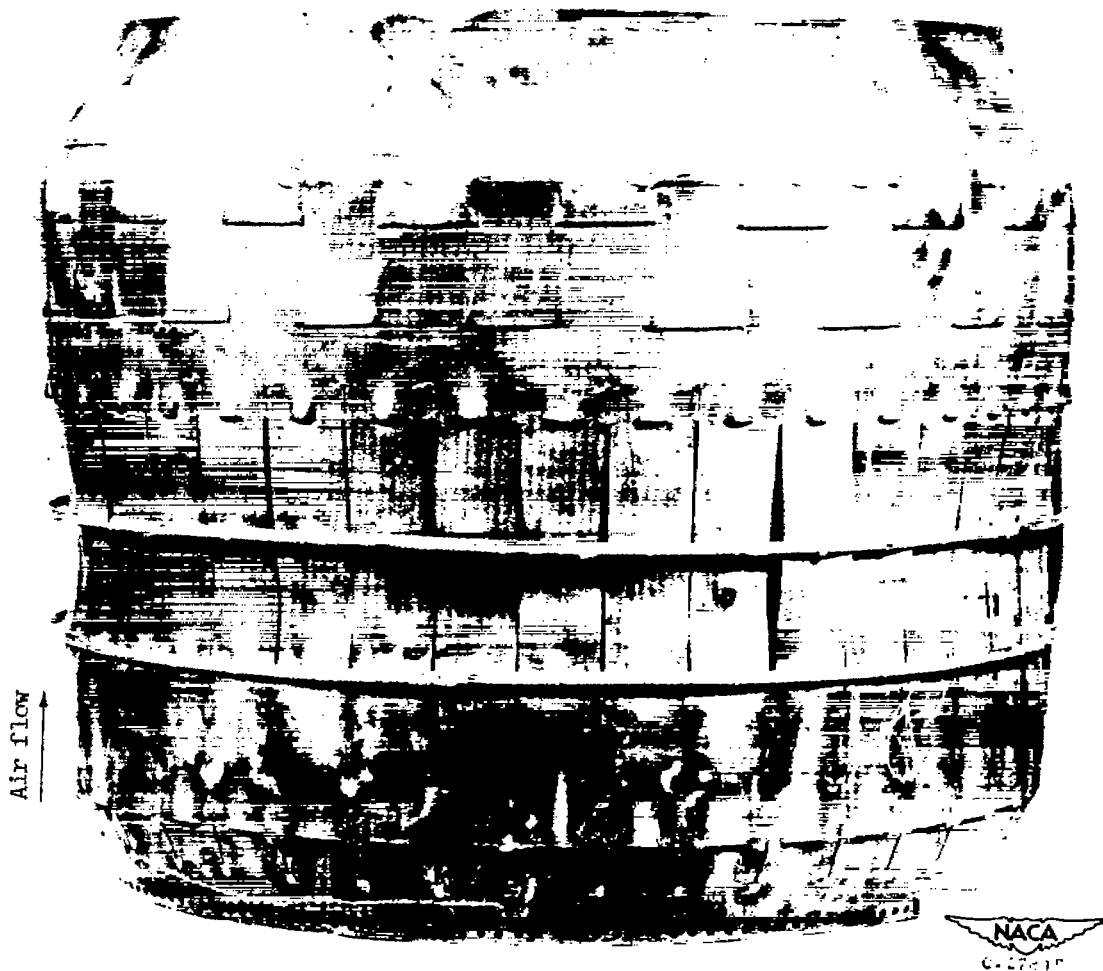
2397



(a) Combustor-outlet quarter view.

Figure 10. - NACA combustor model 6 after 108 hours of operation.





(b) Combustor side view.

Figure 10. - Concluded. NACA combustor model 6 after 108 hours of operation.

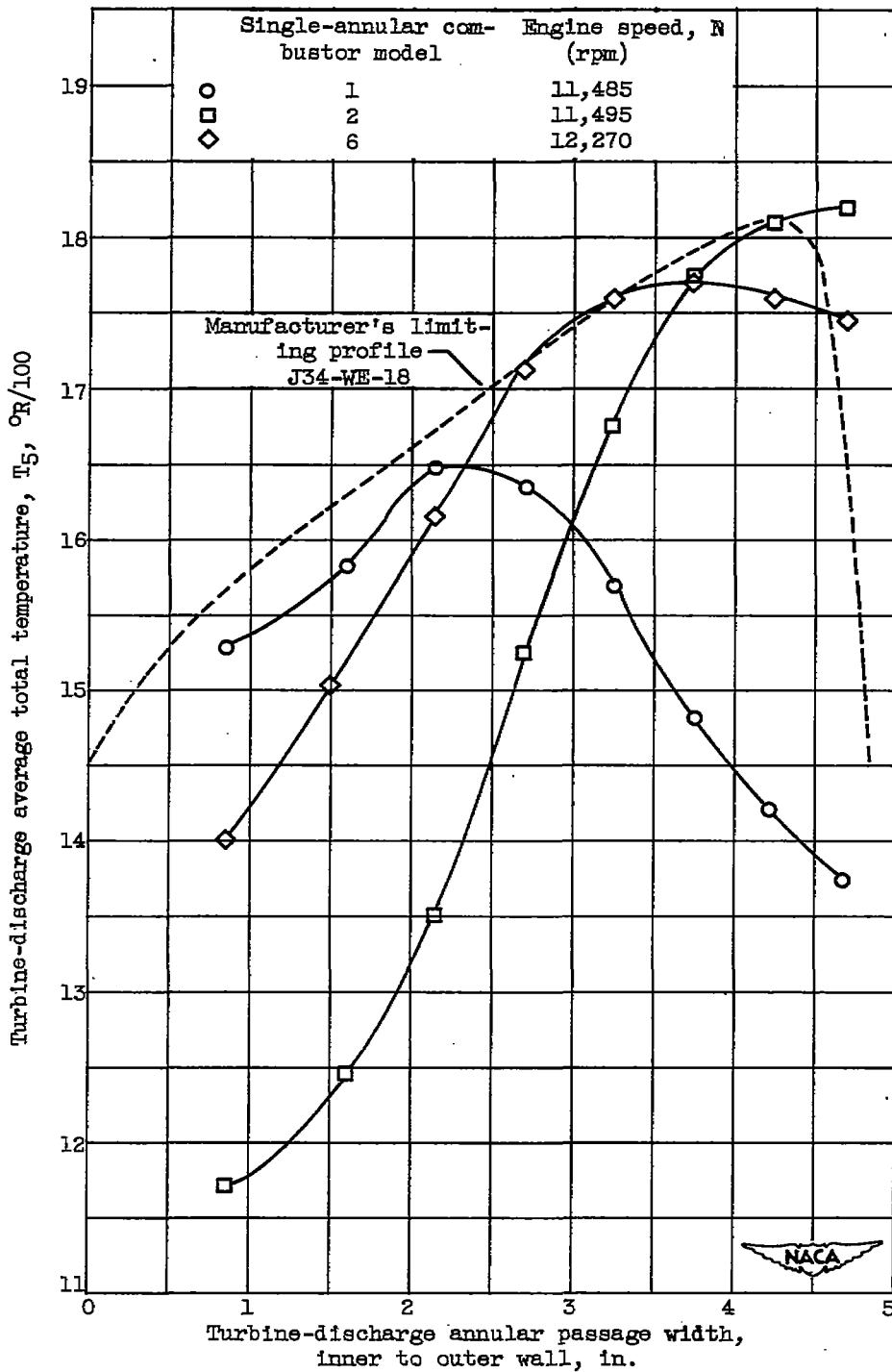
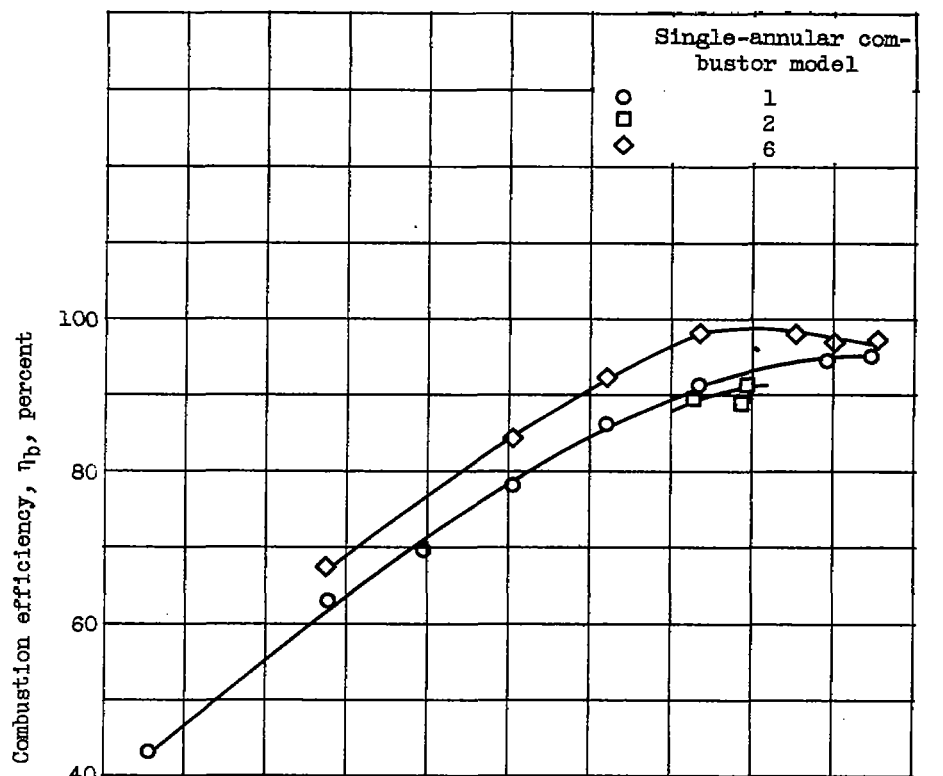
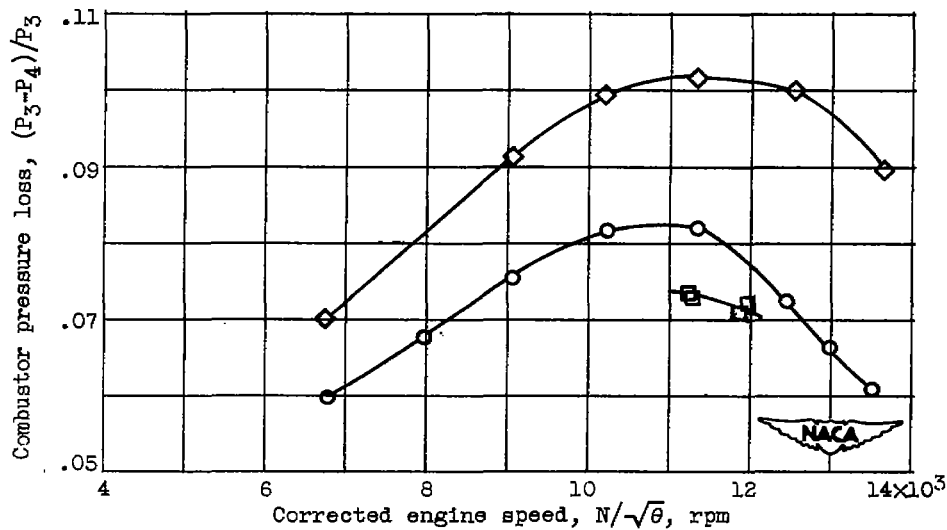


Figure 11. - Effect of combustor-design modifications on turbine-discharge temperature profiles of single-annular combustor with 6.0-gallon-per-hour fuel nozzles at altitude of 40,000 feet and flight Mach number of 0.30.



(a) Combustion efficiency.



(b) Combustor pressure loss.

Figure 12. - Effect of combustor-design modifications on combustion efficiency and pressure loss of single-annular combustor with 6.0-gallon-per-hour fuel nozzles at altitude of 40,000 feet and flight Mach number of 0.30.

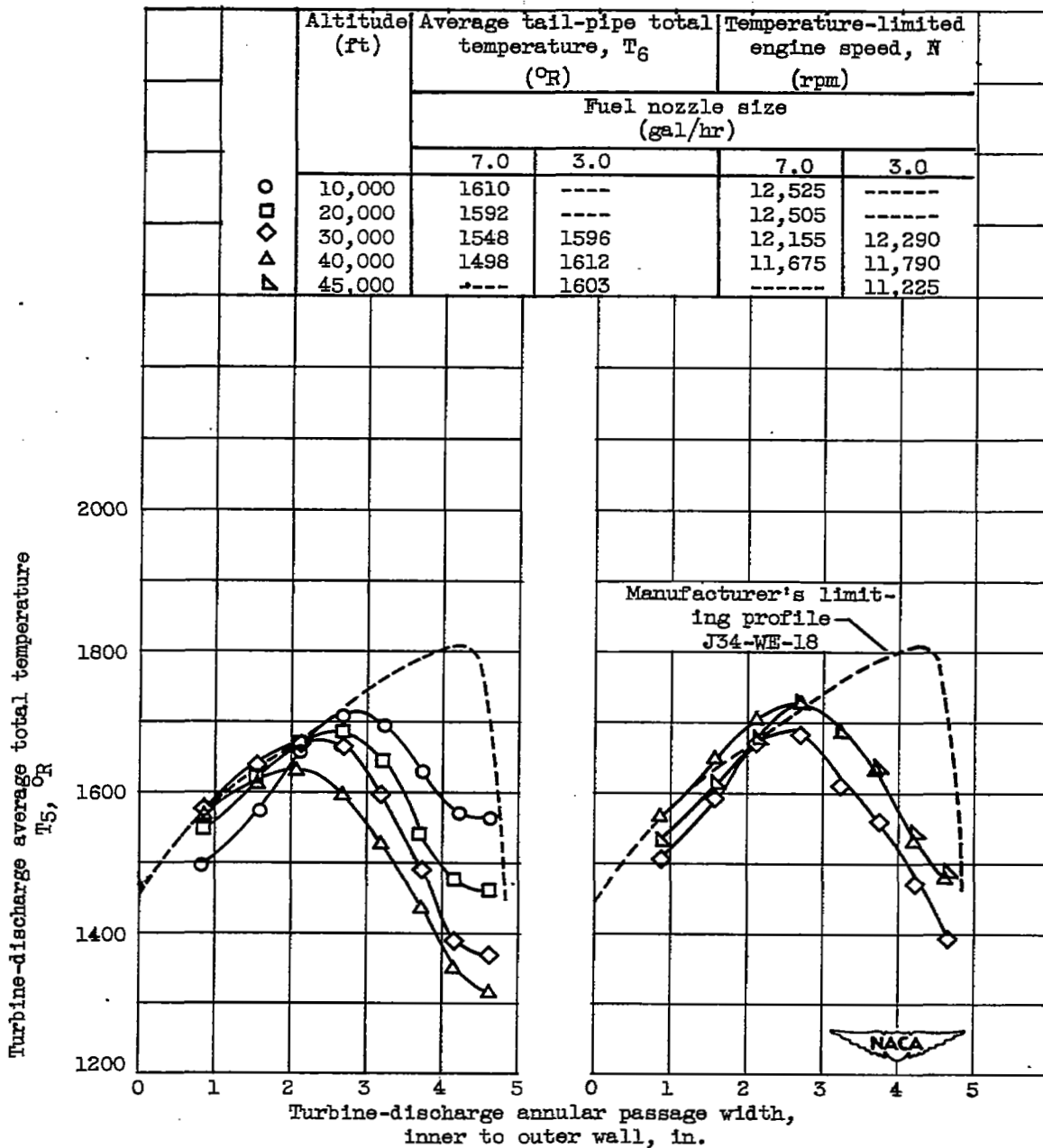
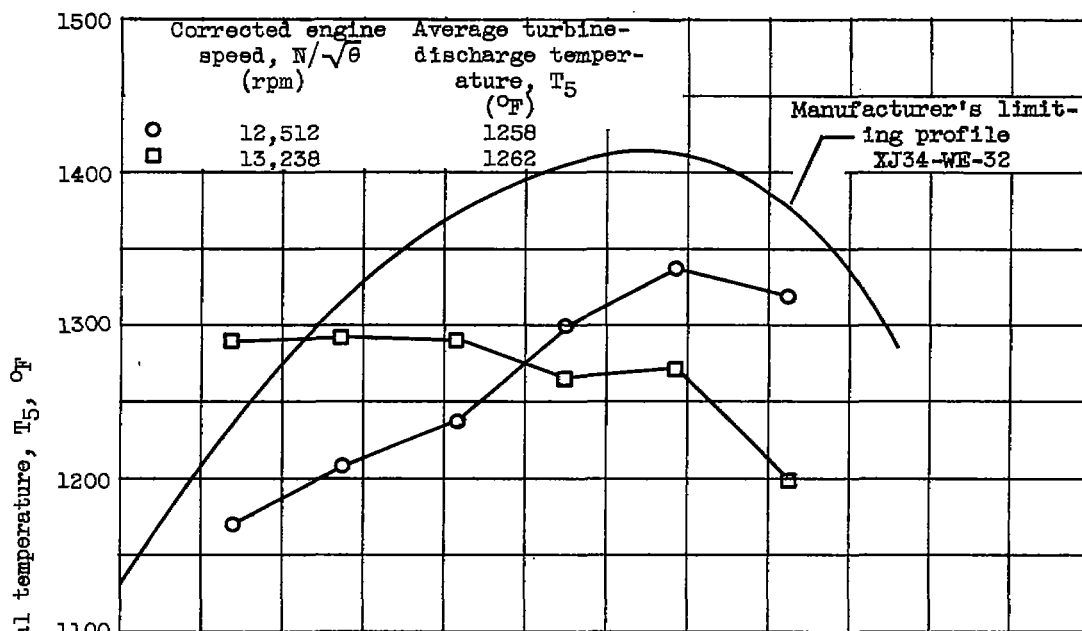
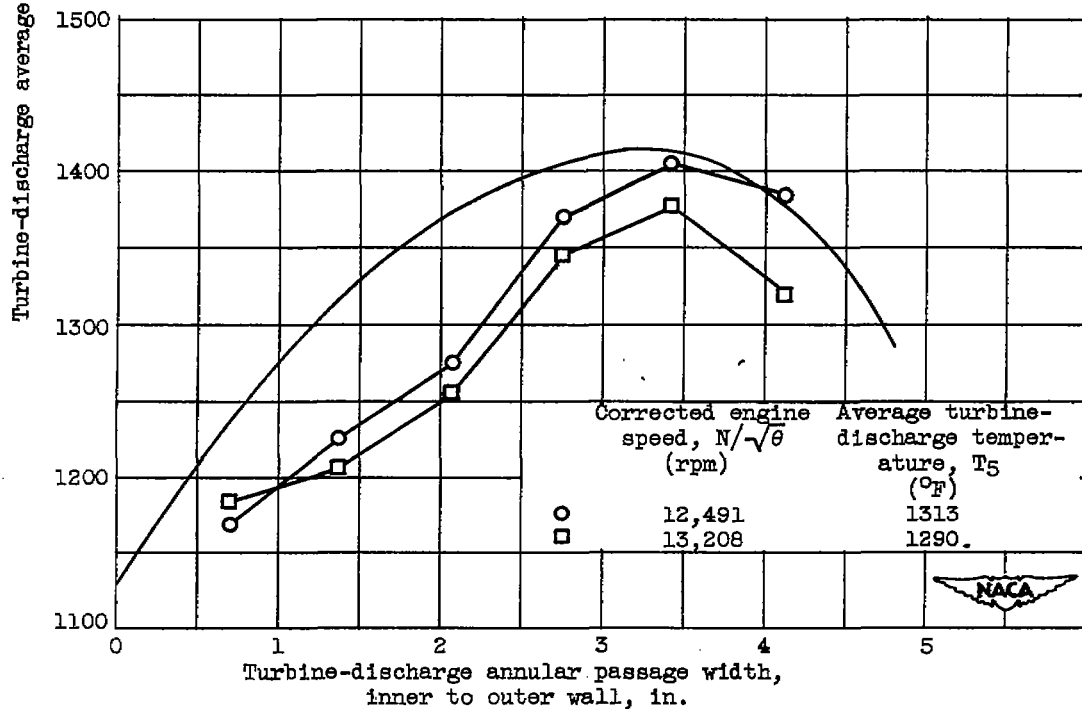


Figure 13. - Effect of fuel-nozzle size on turbine-discharge temperature profiles of double-annular combustor at flight Mach number of 0.30 and maximum temperature-limited engine speed.



(a) Without mixer.



(b) With mixer.

Figure 14. - Effect of flow mixer on turbine-discharge temperature profiles of XJ34-WE-32 turbojet engine equipped with variable-area exhaust nozzle. Altitude, 25,000 feet; Mach number, 0.52.

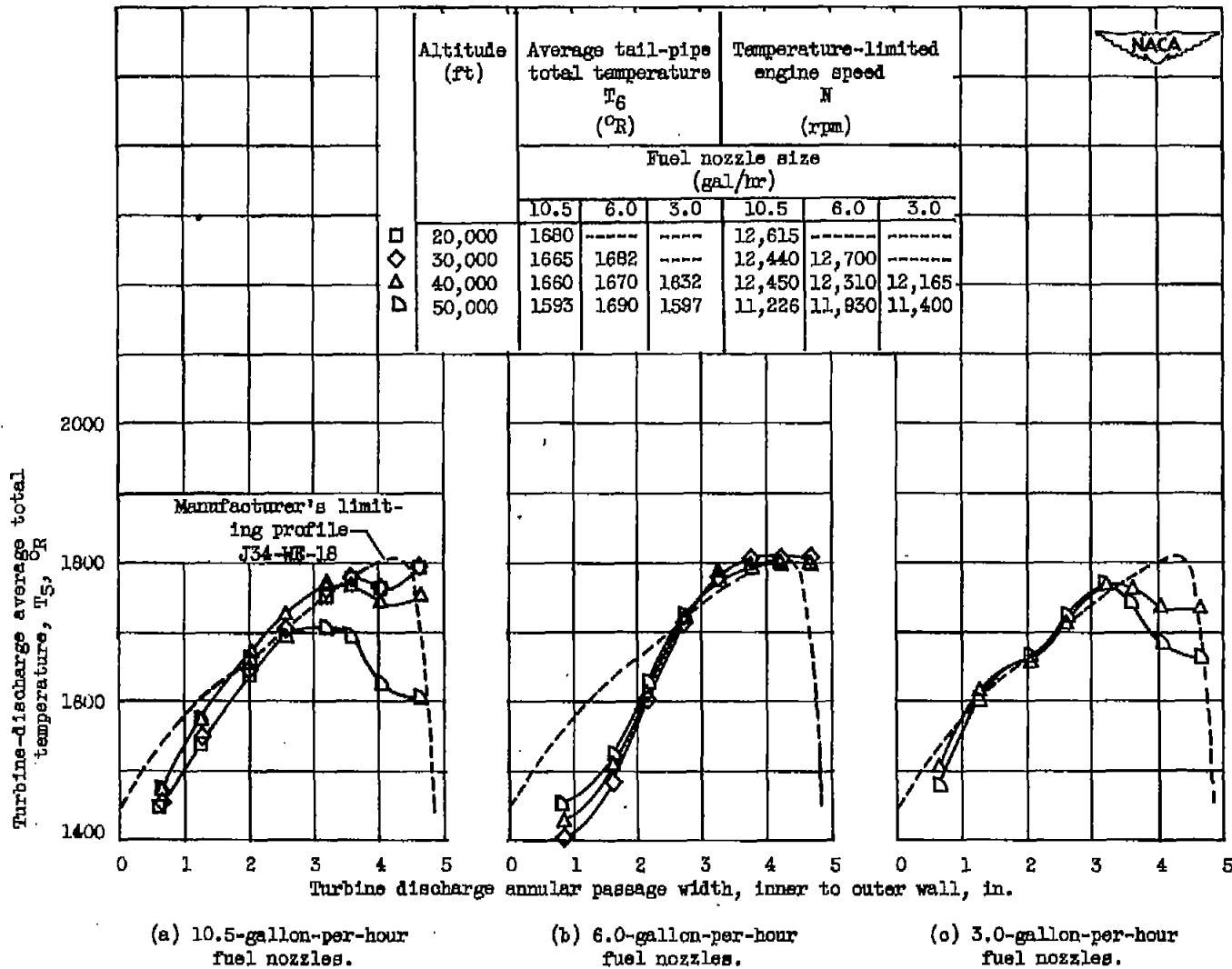


Figure 15. - Effect of fuel nozzle size on turbine-discharge temperature profiles of single-annular combustor at flight Mach number of 0.60 and maximum temperature-limited engine speed.

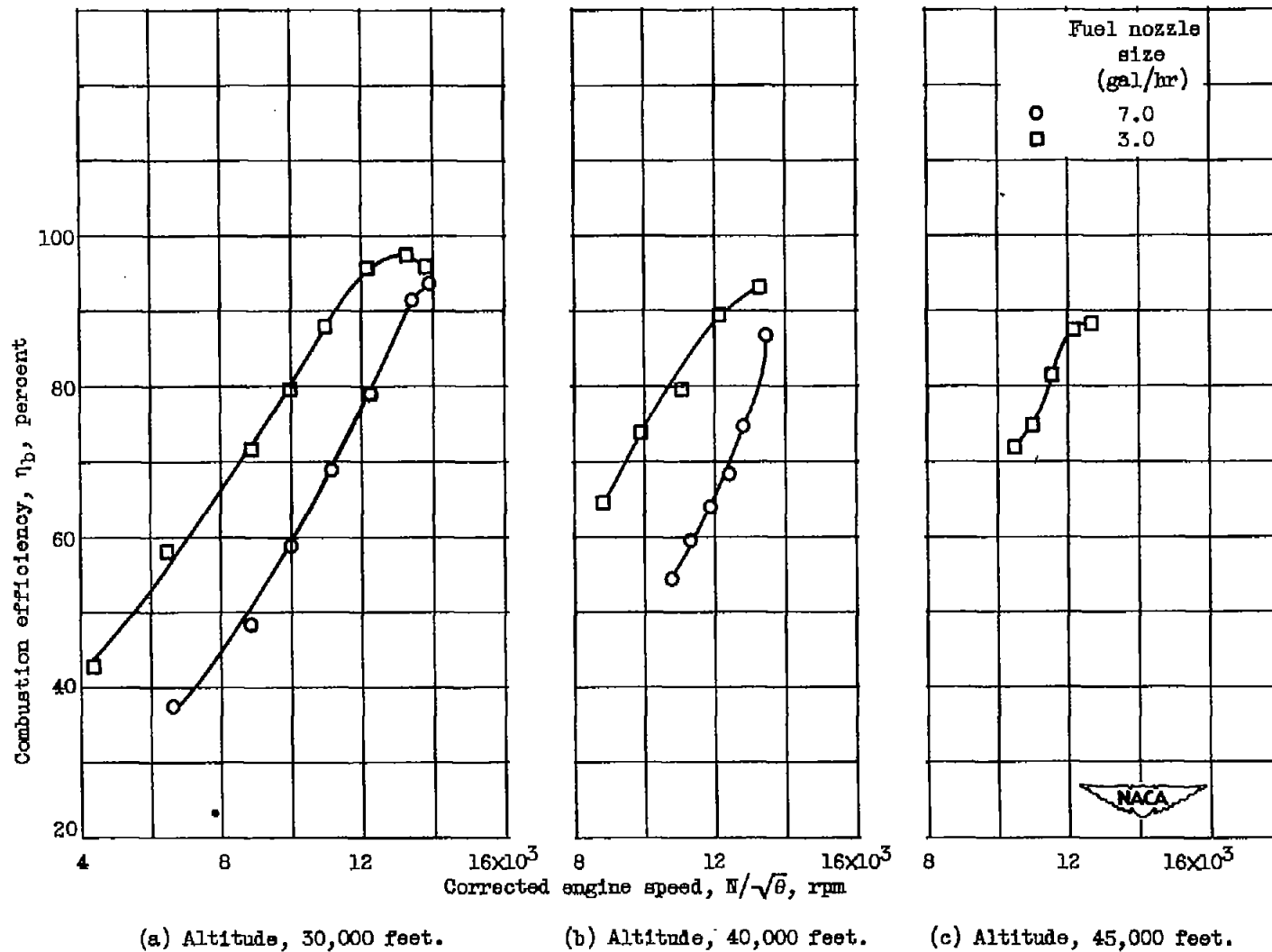
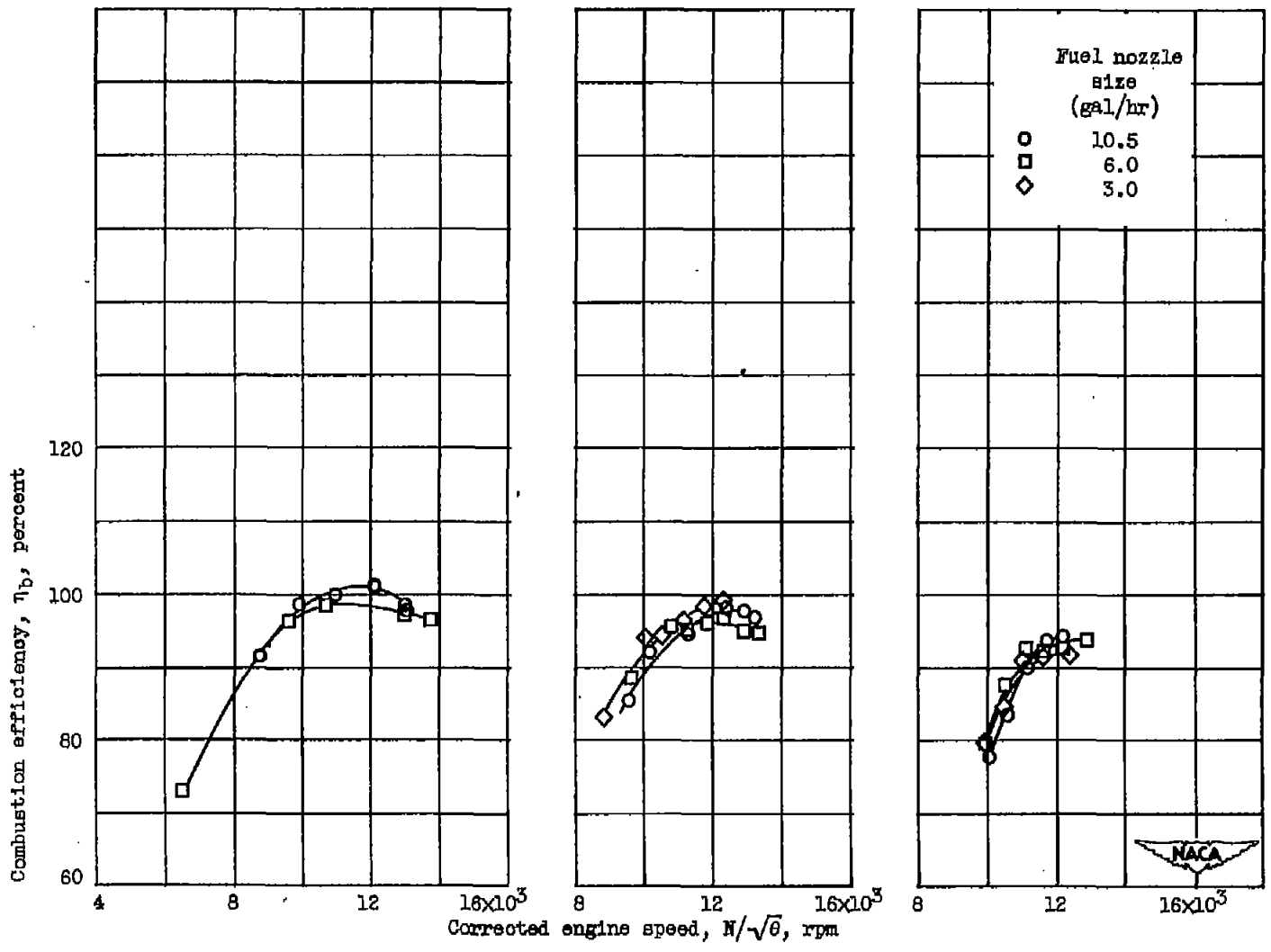
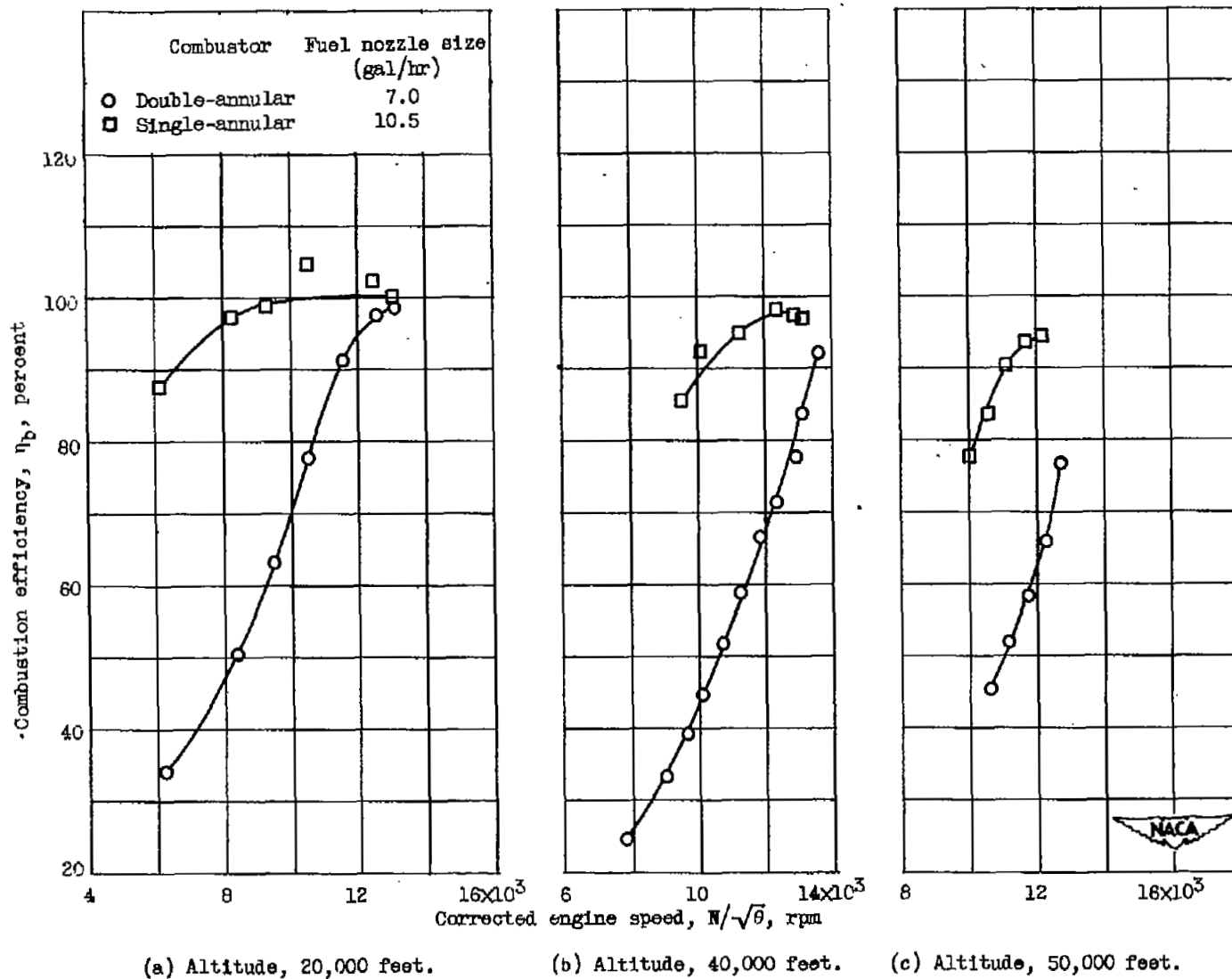


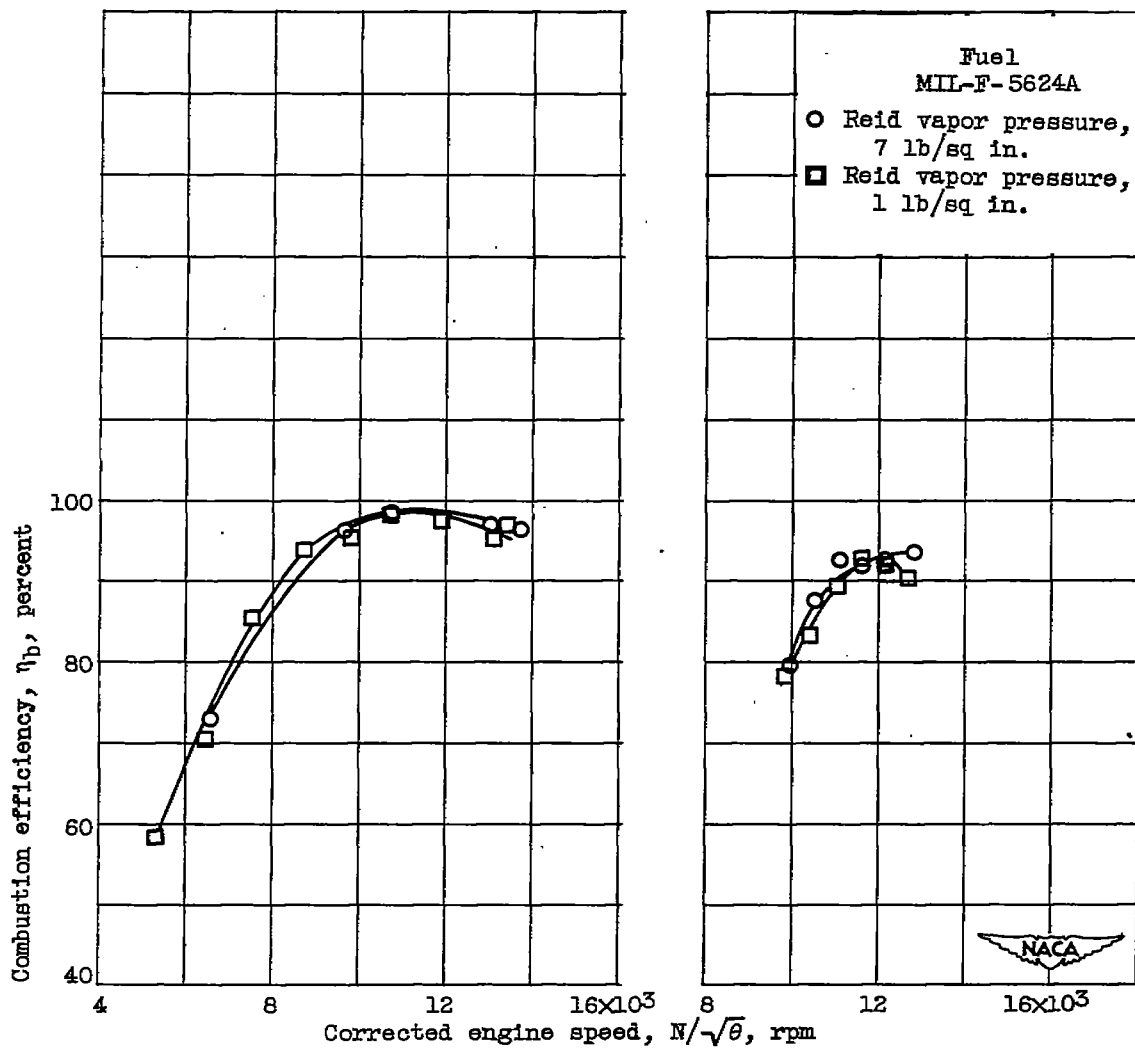
Figure 16. - Effect of fuel nozzle size on combustion efficiency of double-annular combustor at flight Mach number of 0.30.



(a) Altitude, 30,000 feet. (b) Altitude, 40,000 feet. (c) Altitude, 50,000 feet.

Figure 17. - Effect of fuel nozzle size on combustion efficiency of single-annular combustor at flight Mach number of 0.60.





(a) Altitude, 30,000 feet.

(b) Altitude, 50,000 feet.

Figure 19. - Effect of two fuels of different Reid vapor pressures on combustion efficiency of single-annular combustor at flight Mach number of 0.60 using 6.0-gallon-per-hour fuel nozzles.

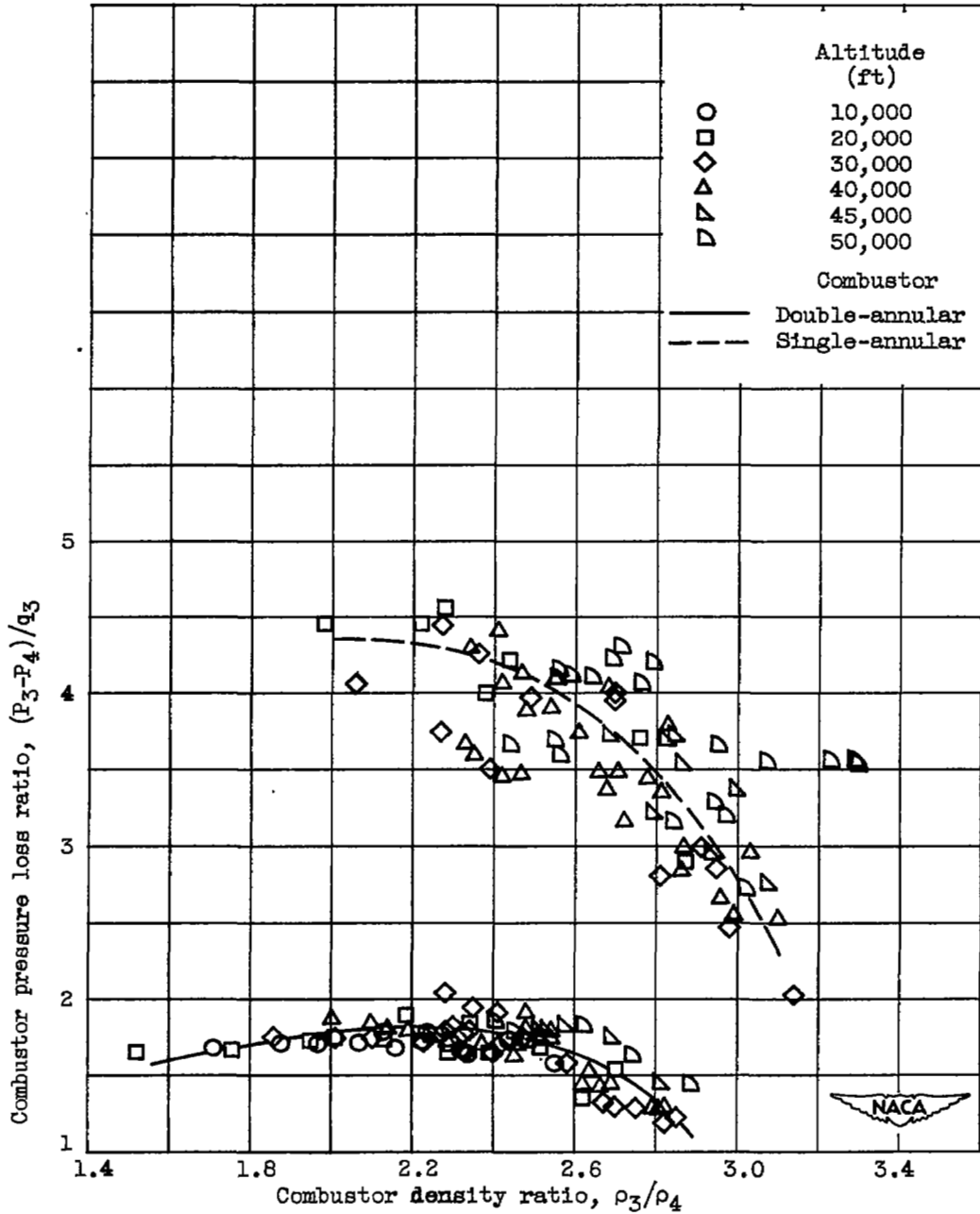


Figure 20. - Comparison of combustor pressure loss of single- and double-annular combustors.

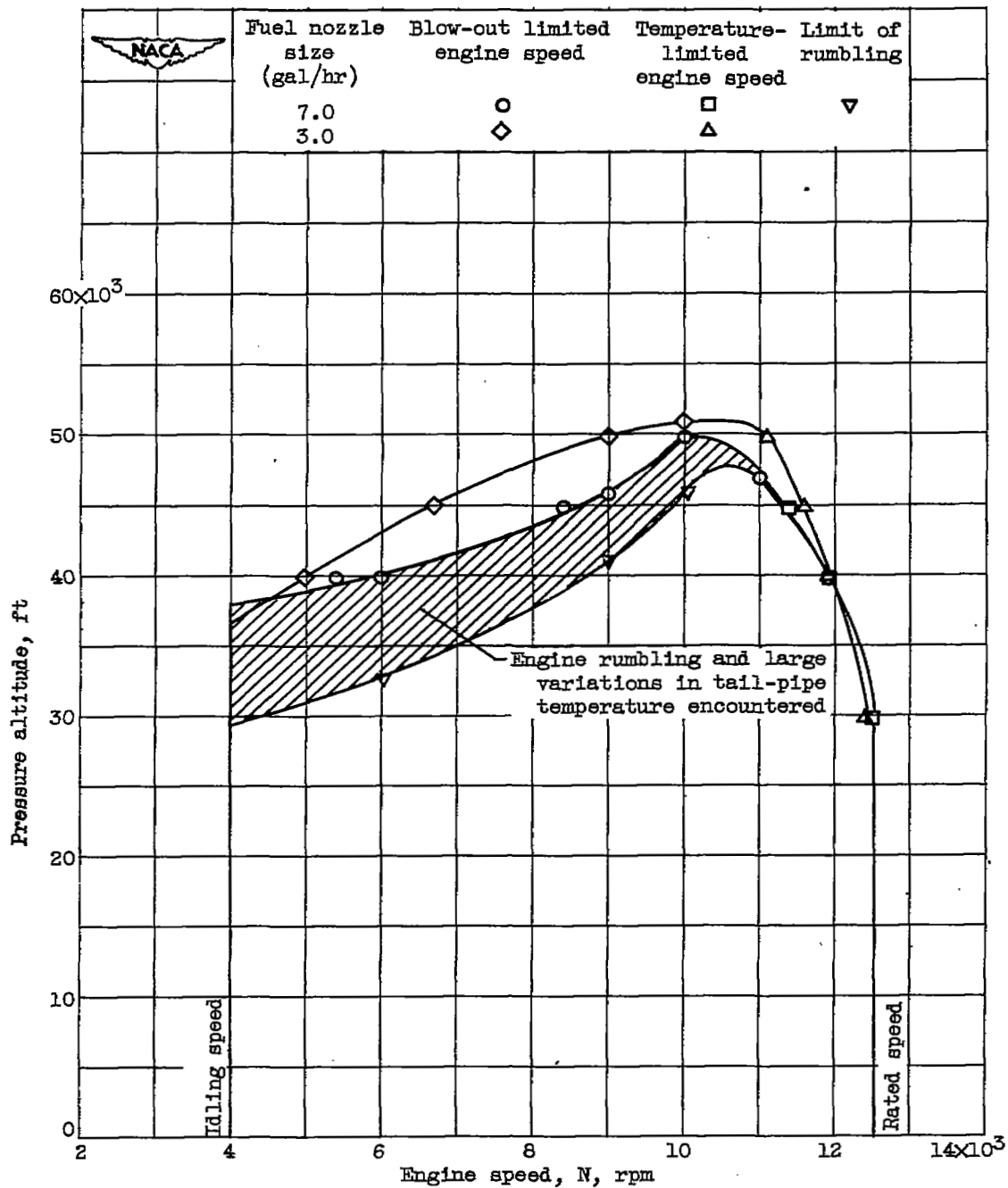


Figure 21. - Effect of fuel nozzle size on altitude limits of double-annular combustor at flight Mach number of 0.30.

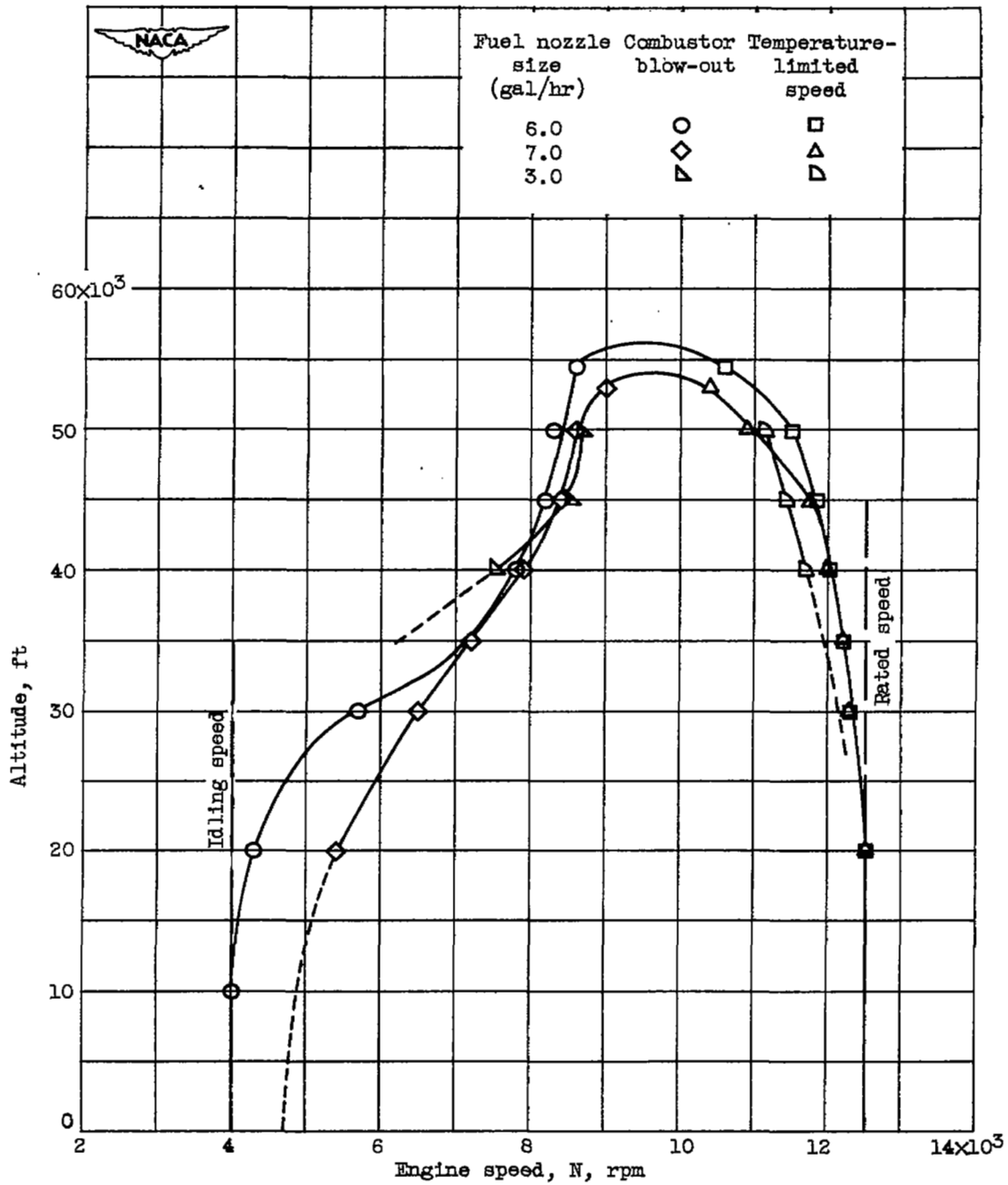


Figure 22. - Effect of fuel nozzle size on altitude limits of single-annular combustor at flight Mach number of 0.60.

2397

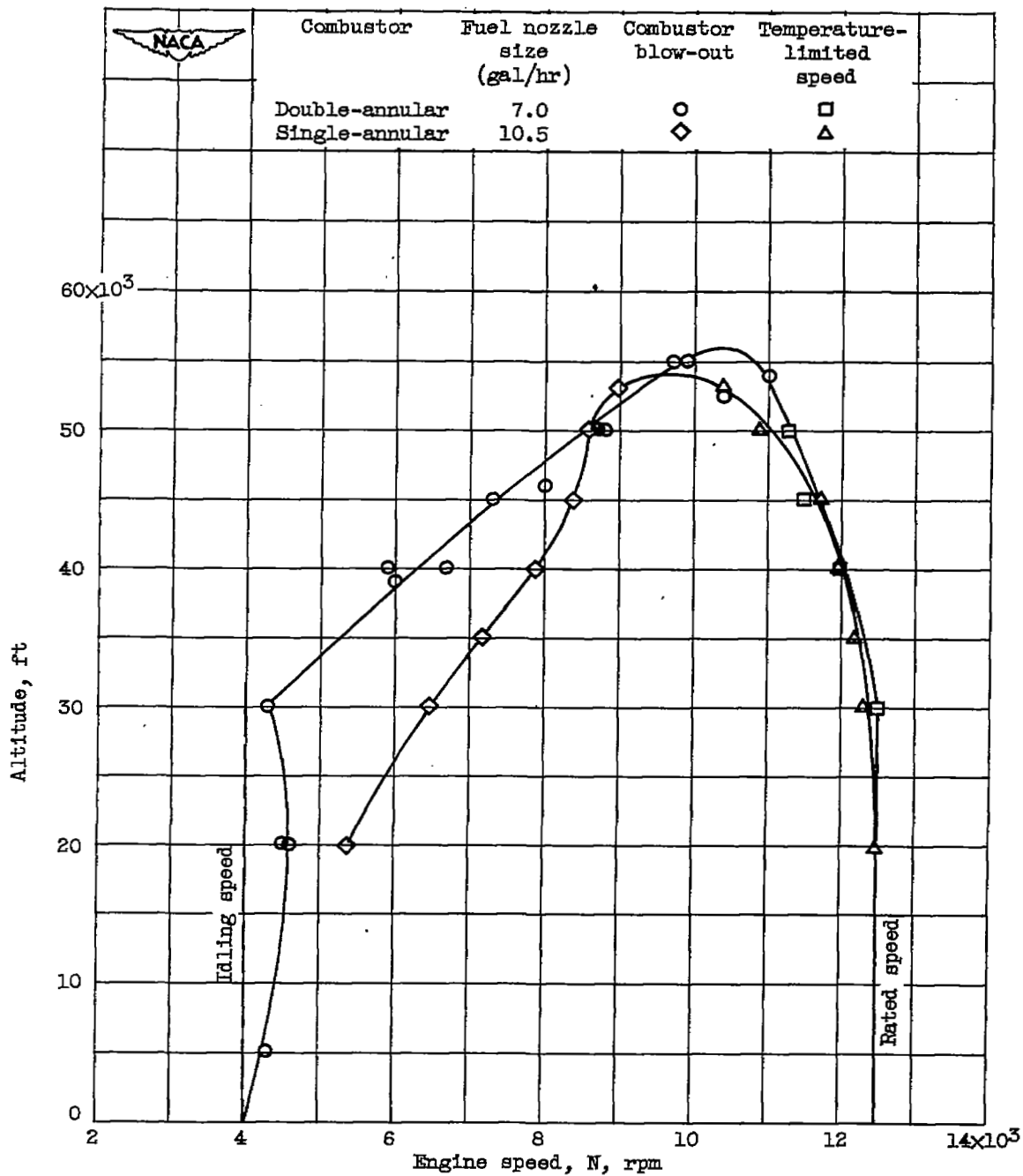


Figure 23. - Comparison of altitude limits of single- and double-annular combustors at flight Mach number of 0.60.

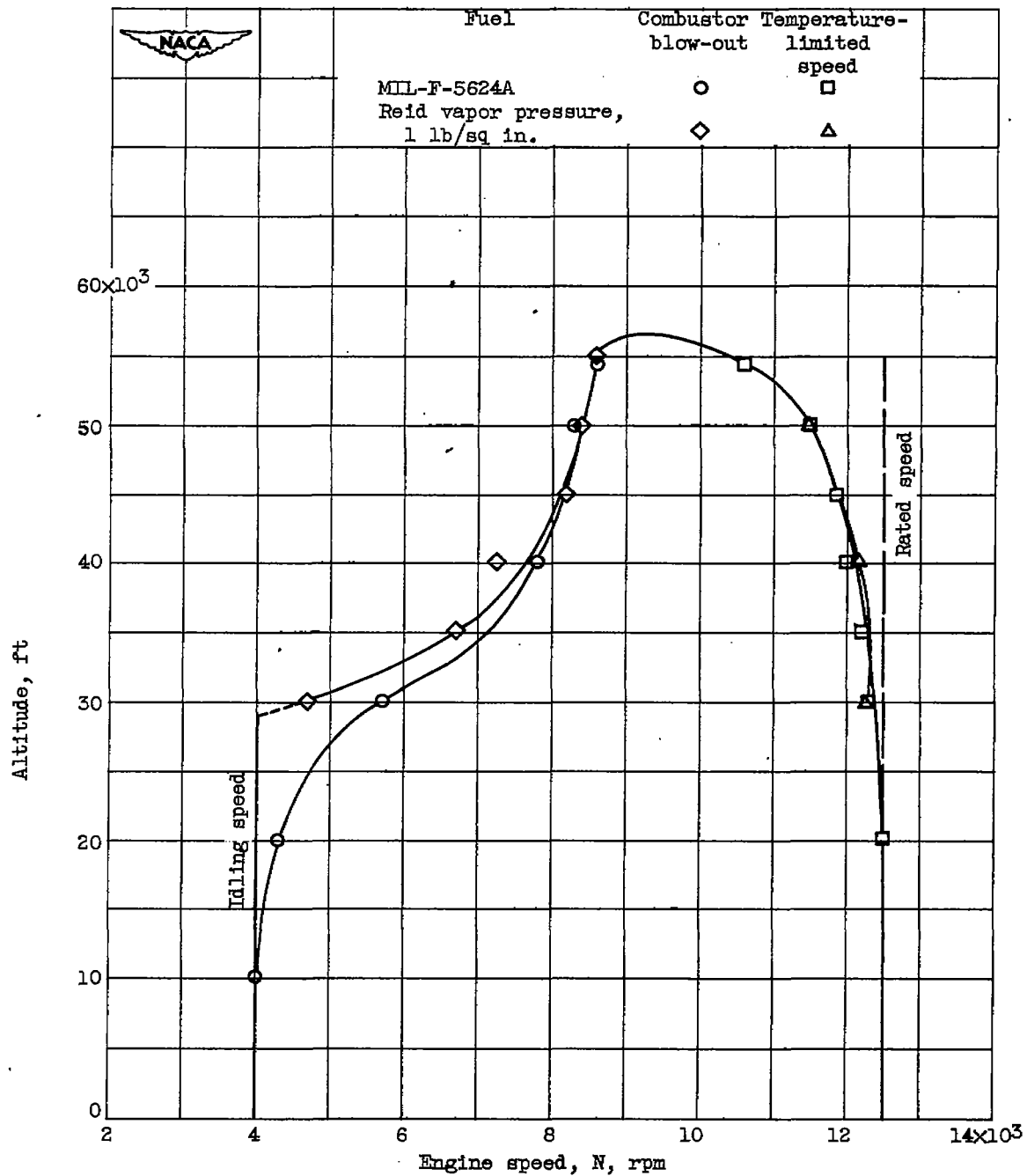
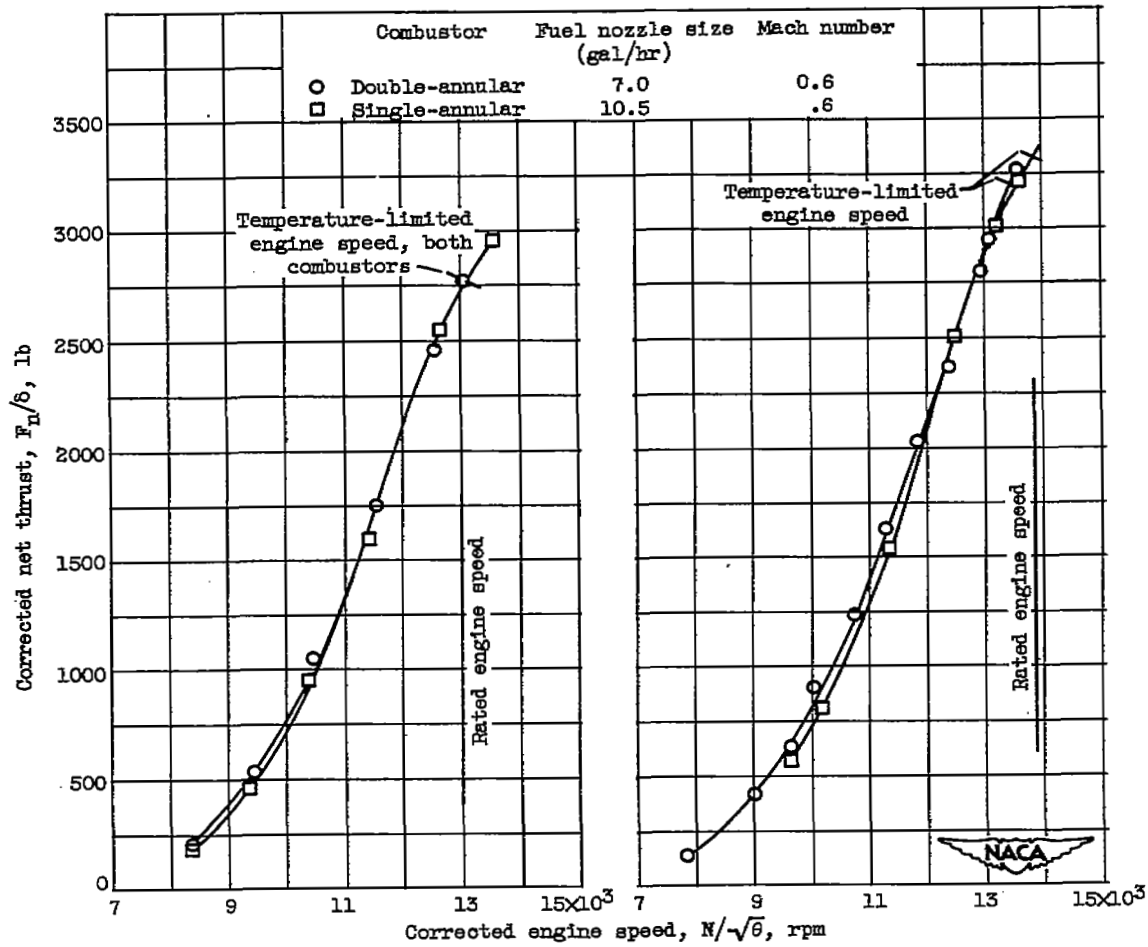


Figure 24. - Effect of two fuels of different Reid vapor pressures on altitude limits of single-annular combustor with 6.0-gallon-per-hour fuel nozzles at flight Mach number of 0.60.

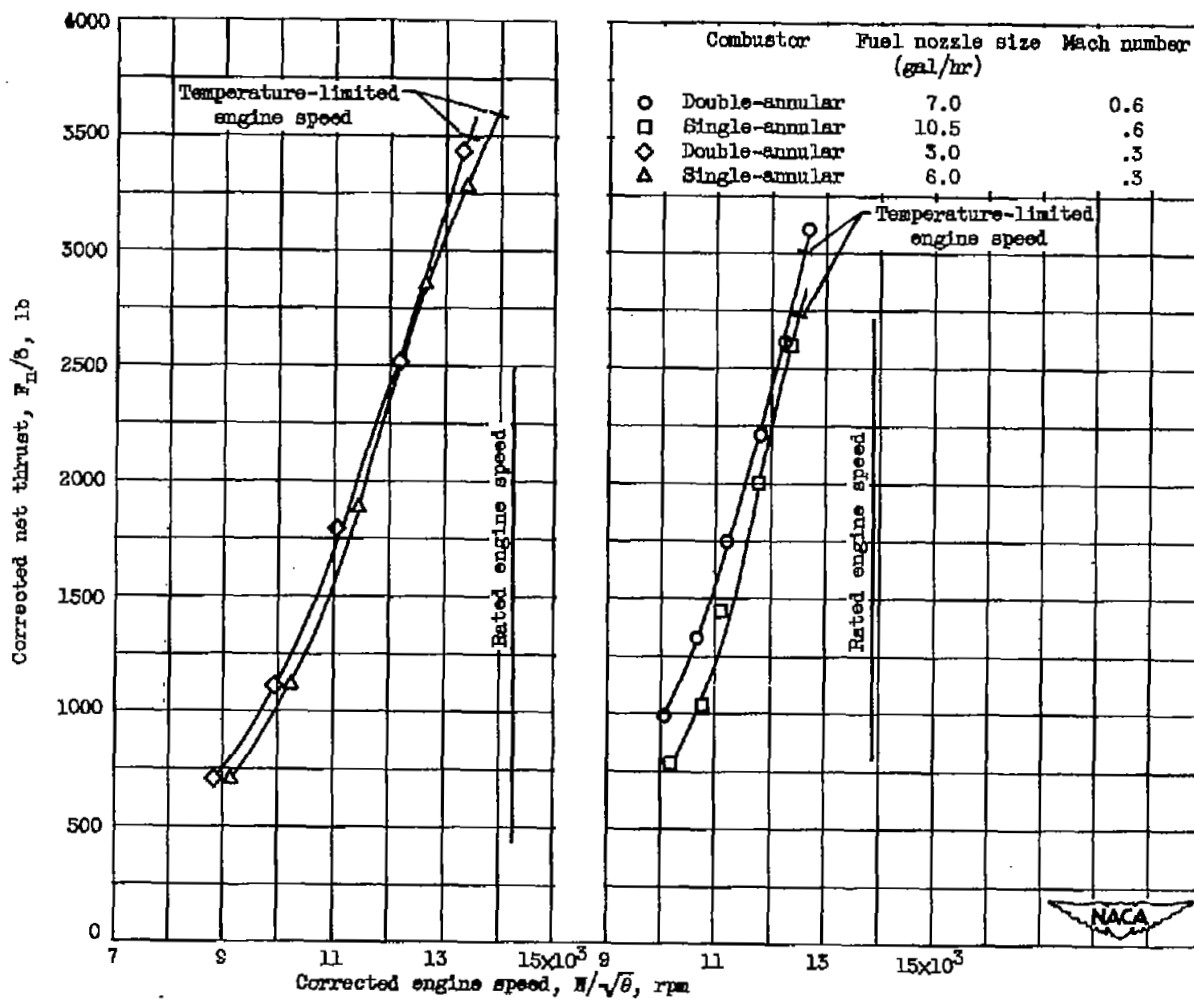
2397



(a) Altitude, 20,000 feet;
Mach number, 0.60.

(b) Altitude, 40,000 feet;
Mach number, 0.60.

Figure 25. - Comparison of corrected net thrust of single- and double-annular combustors at several altitudes, Mach numbers, and fuel nozzle sizes.



(a) Altitude, 40,000 feet;
Mach number, 0.30.

(d) Altitude, 50,000 feet;
Mach number, 0.60.

Figure 25. - Concluded. Comparisons of corrected net thrust of single- and double-annular combustors at several altitudes, Mach numbers, and fuel nozzle sizes.

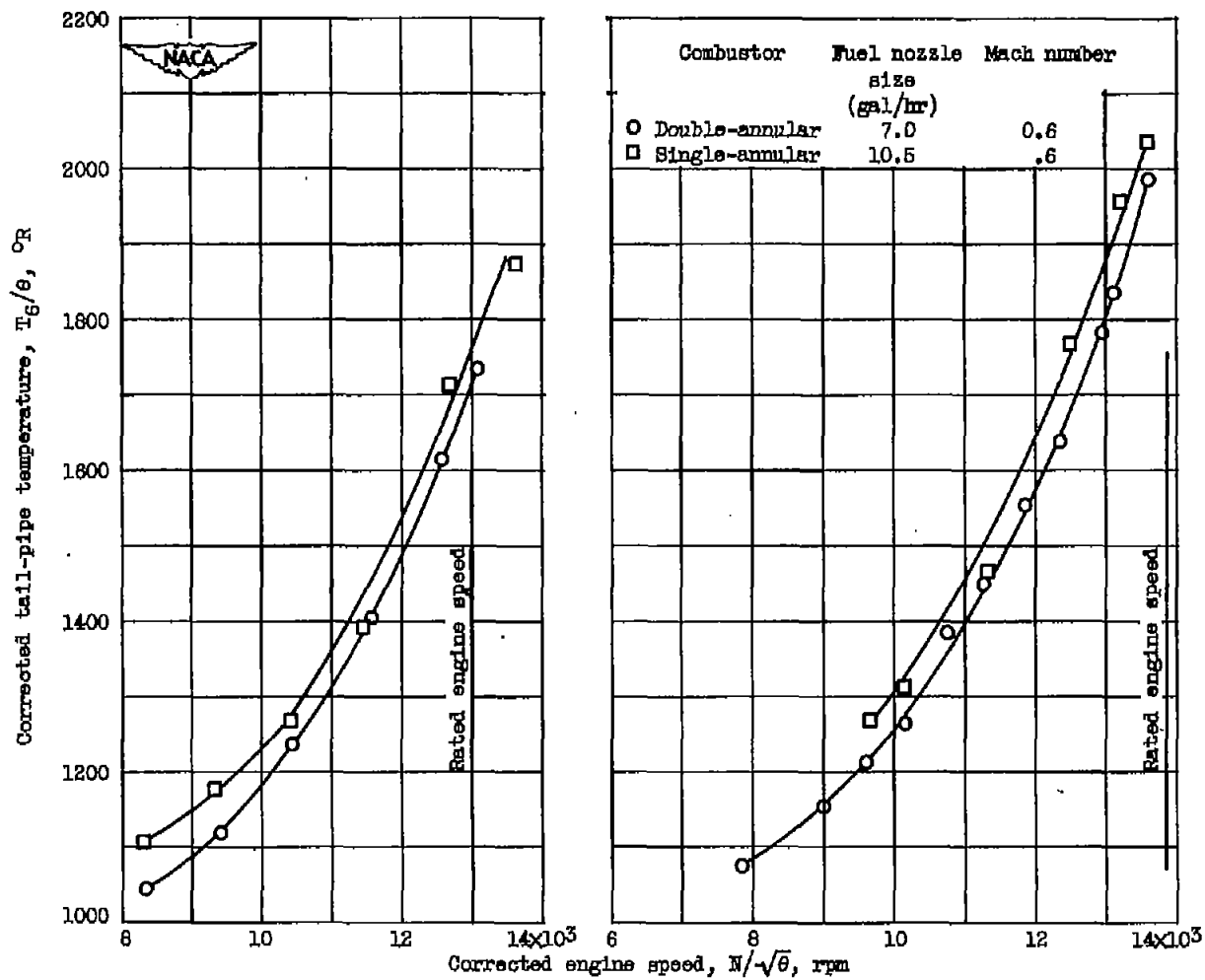


Figure 26. - Comparison of corrected tail-pipe temperature of single- and double-annular combustors at several altitudes, Mach numbers, and fuel nozzle sizes.

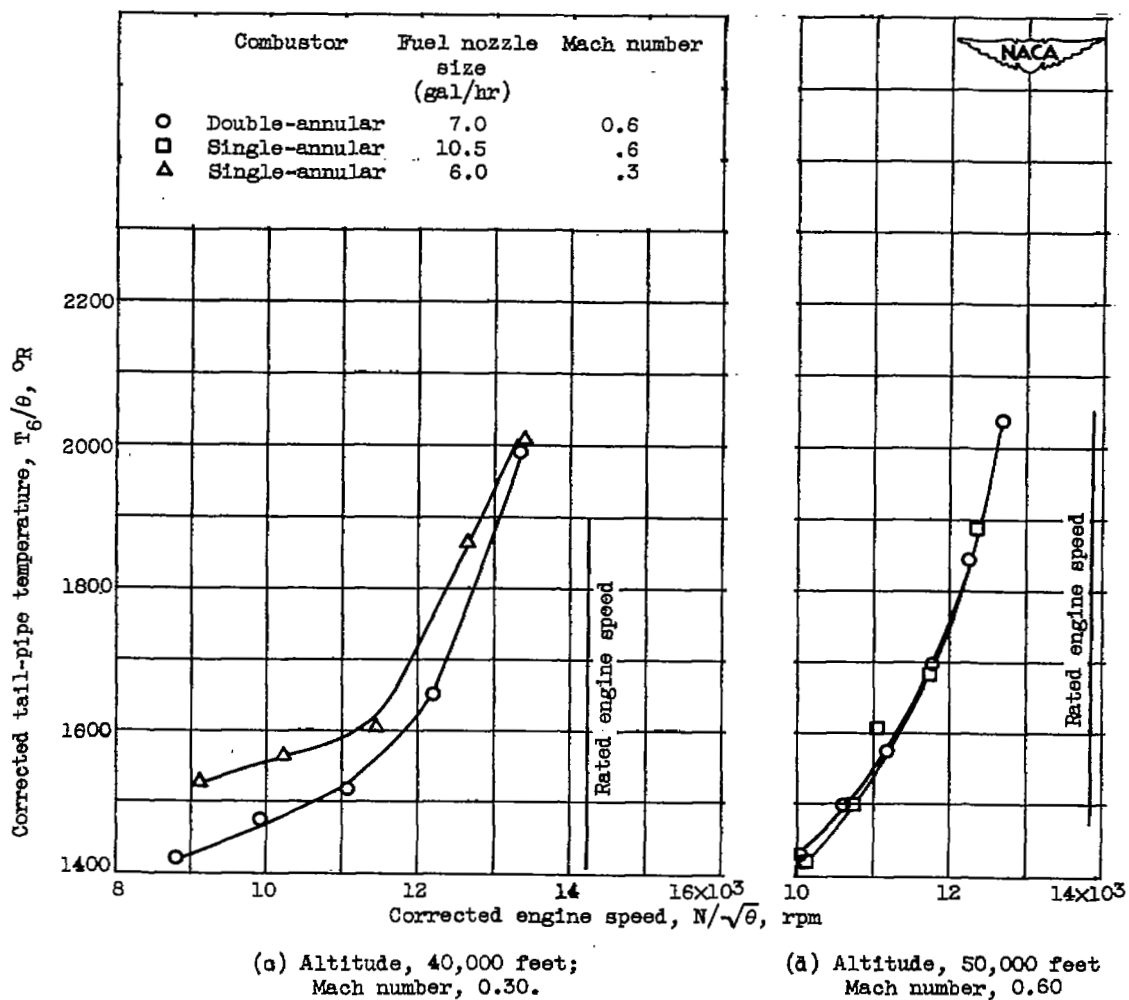


Figure 26. - Concluded. Comparison of corrected tail-pipe temperature of single- and double-annular combustors at several altitudes, Mach numbers, and fuel nozzle sizes.

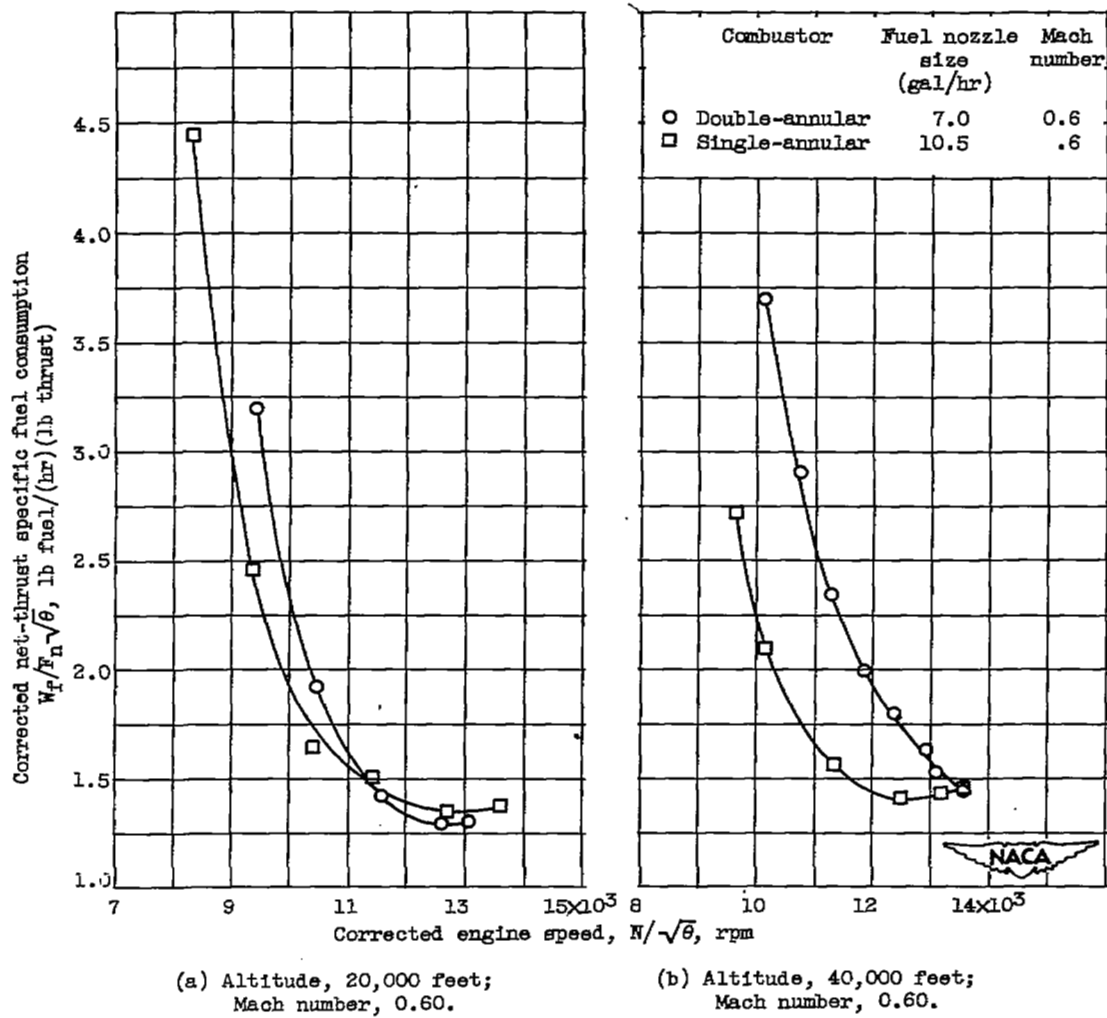


Figure 27. - Comparison of net-thrust specific fuel consumption of single- and double-annular combustors at several altitudes, Mach numbers, and fuel nozzle sizes.

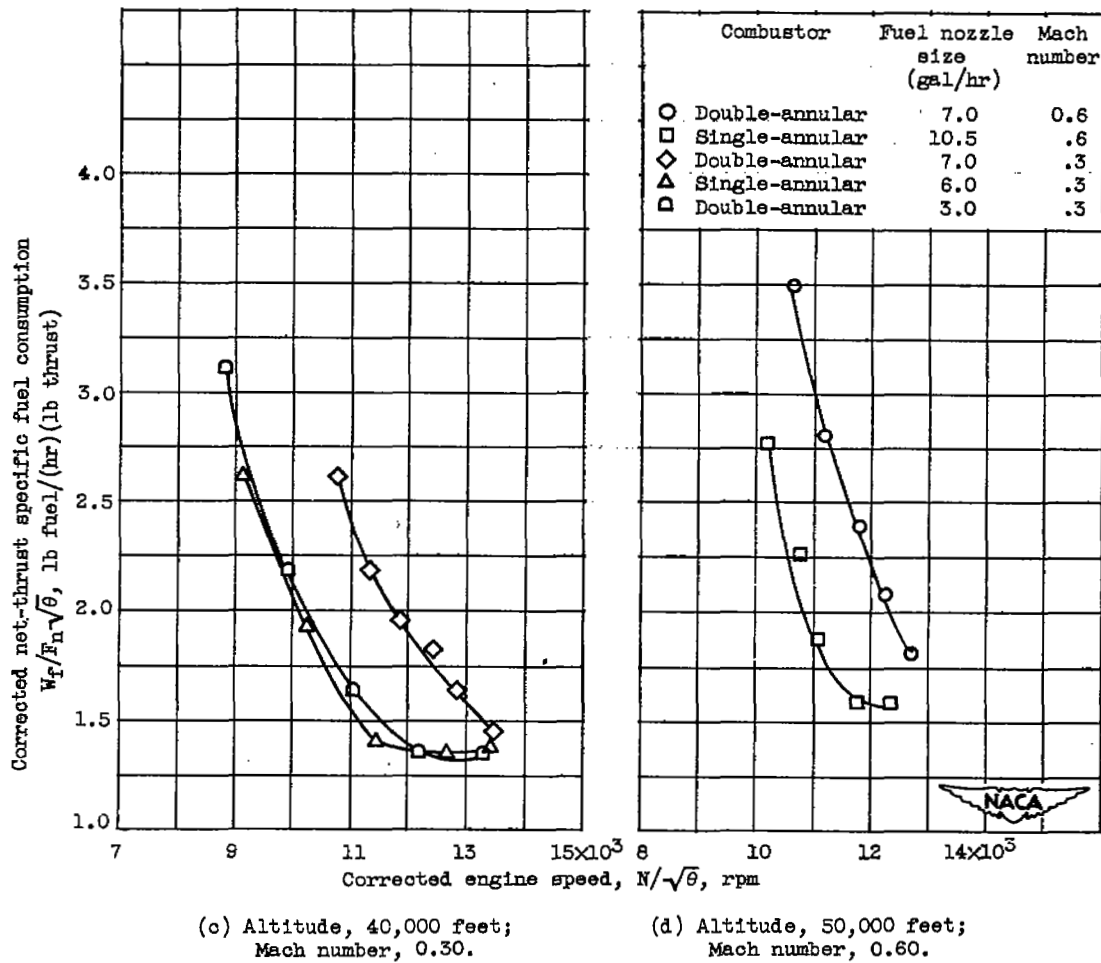
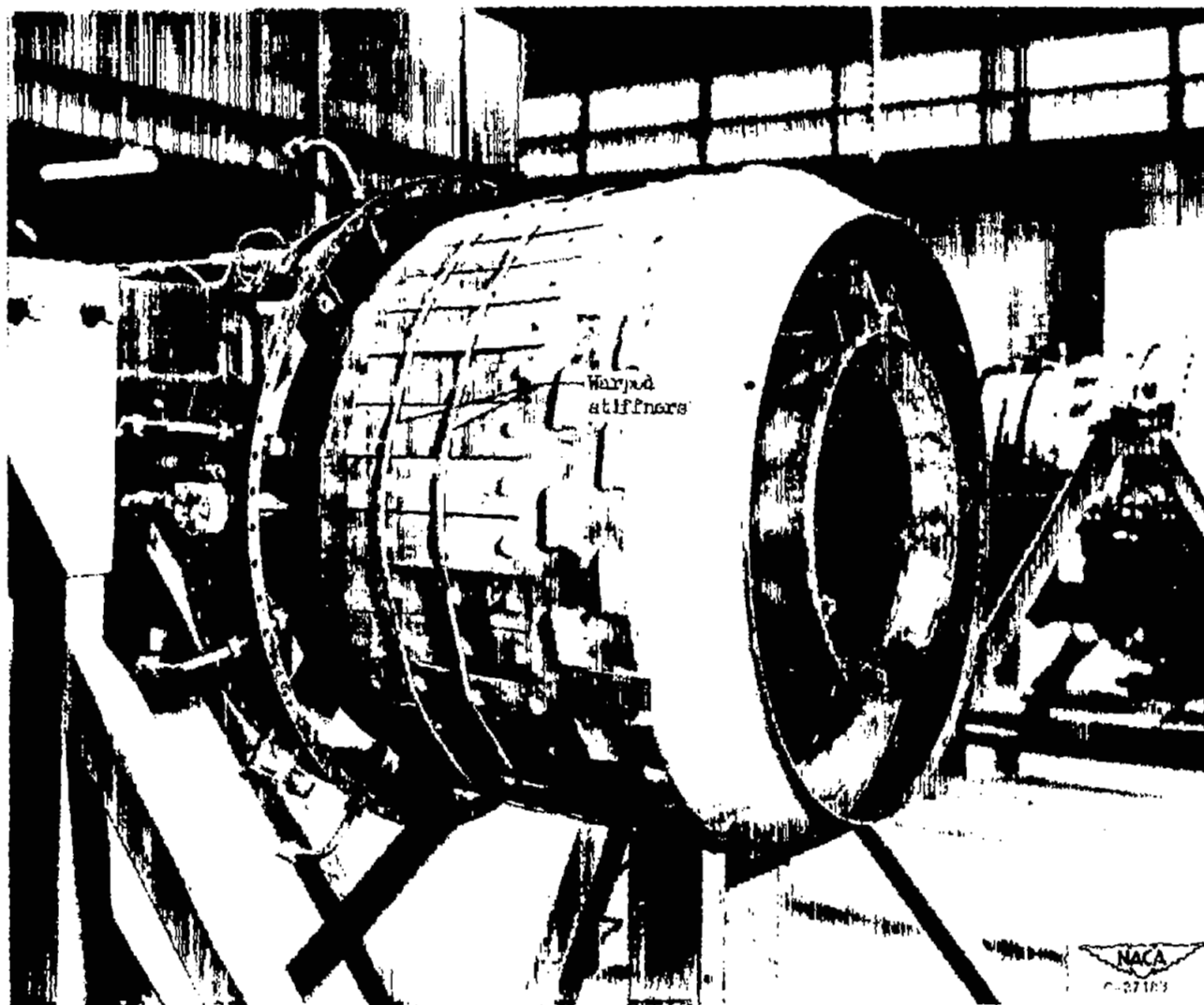


Figure 27. - Concluded. Comparison of net-thrust specific fuel consumption of single- and double-annular combustors at several altitudes, Mach numbers, and fuel nozzle sizes.



(a) Side view of combustor showing warping of liner.

Figure 28. - Warping and carbon deposits on NACA combustor.



(b) Looking upstream at fuel nozzles and carbon deposits.

Figure 28. - Concluded. Warping and carbon deposits on NACA combustor.

SECURITY INFORMATION

NASA Technical Library



3 1176 01434 9832

